

Summer 2010

# Experimental evolution of *Burkholderia cenocepacia* biofilm populations

Steffen R. Poltak

*University of New Hampshire, Durham*

Follow this and additional works at: <https://scholars.unh.edu/dissertation>

---

## Recommended Citation

Poltak, Steffen R., "Experimental evolution of *Burkholderia cenocepacia* biofilm populations" (2010). *Doctoral Dissertations*. 534.  
<https://scholars.unh.edu/dissertation/534>

This Dissertation is brought to you for free and open access by the Student Scholarship at University of New Hampshire Scholars' Repository. It has been accepted for inclusion in Doctoral Dissertations by an authorized administrator of University of New Hampshire Scholars' Repository. For more information, please contact [nicole.hentz@unh.edu](mailto:nicole.hentz@unh.edu).

EXPERIMENTAL EVOLUTION OF BURKHOLDERIA CENOCEPACIA BIOFILM  
POPULATIONS

By

STEFFEN R. POLTAK

BA Saint Anselm College, 2003

DISSERTATION

Submitted to the University of New Hampshire

in partial fulfillment of

the Requirements for the Degree of

Doctor of Philosophy

in

Microbiology

UMI Number: 3430788

All rights reserved

**INFORMATION TO ALL USERS**

The quality of this reproduction is dependent upon the quality of the copy submitted.

In the unlikely event that the author did not send a complete manuscript and there are missing pages, these will be noted. Also, if material had to be removed, a note will indicate the deletion.



UMI 3430788

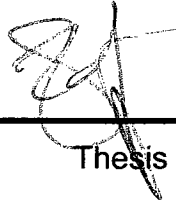
Copyright 2010 by ProQuest LLC.

All rights reserved. This edition of the work is protected against unauthorized copying under Title 17, United States Code.



ProQuest LLC  
789 East Eisenhower Parkway  
P.O. Box 1346  
Ann Arbor, MI 48106-1346

This thesis has been examined and approved.



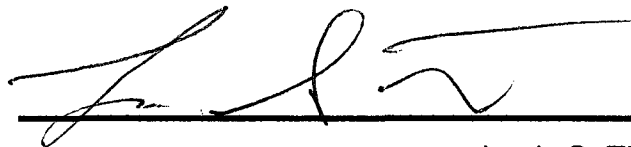
---

Thesis Director, Vaughn S. Cooper,  
Associate Professor, MCBS



---

Cheryl A. Whistler,  
Assistant Professor, MCBS



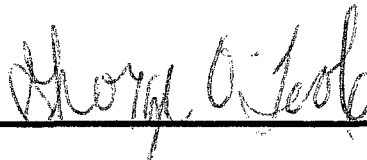
---

Louis S. Tisa,  
~~Associate~~ Professor, MCBS



---

William Kelley Thomas,  
Professor, MCBS



---

George A. O'Toole,  
Associate Professor, Department of Microbiology and Immunology,  
Dartmouth Medical School

---

8/23/10

Date

## TABLE OF CONTENTS

ACKNOWLEDGMENTS.....	iii
LIST OF TABLES.....	iv
LIST OF FIGURES.....	v
ABSTRACT.....	vii

CHAPTER	PAGE
I. INTRODUCTION .....	8
II. ECOLOGICAL SUCCESSION IN LONG-TERM EXPERIMENTALLY EVOLVED BIOFILMS PRODUCES SYNERGISTIC COMMUNITIES.....	15
III. ORIGINS AND MAINTENANCE OF DIVERSITY IN EVOLVING BIOFILMS: COMPETITION OR FACILITATION?.....	49
IV. EVOLUTIONARY GENETICS OF BIOFILM ADAPTATION BY <i>BURKHOLDERIA CENOCEPACIA</i> .....	79
V. CONCLUSION.....	116
LIST OF REFERENCES.....	119

## **ACKNOWLEDGMENTS**

I would like to thank Vaughn Cooper, George O'Toole, Kelley Thomas, Cheryl Whistler, Elise Sullivan, and Thomas Pistole for their support and guidance. I would also like to thank Robert Mooney, Mark Townley, and Nancy Cherim for their technical support and insight. I would especially like to thank Charles Traverse for all his molecular work on this project, as well as Kenneth Flynn and Jennifer Mahoney for their support and help in proofreading this thesis. Finally, I would like to thank my family and friends for their love and support. This work was made possible through funding by a Hatch grant from the NH Agricultural Experiment Station, the National Institutes of Health grant NIH 1R15AI082528, and the Department of Energy Joint Genome Institute grant JGI CSP-158.

## LIST OF TABLES

<b>CHAPTER IV.</b>	<b>Page</b>
Table 1. Mutations detected by Illumina genome resequencing of a single representative clone of each morphotype following 1500 generations of biofilm experimental evolution.....	87
Table 3. Frequencies of mutant alleles detected in S, R, and W at 1500 generations.....	100
Table 2. Frequencies of mutant alleles detected in S, R, and W at 750 generations.....	100
Table 4. Detection of the <i>yciR</i> gene deletion in replicate experimental biofilm populations after 1500 generations.....	101
Table 5. All mutations detected from Illumina sequencing of population metagenomes and morphotype clones.....	102
Table 6. 95-gene deletion (m2) on chromosome 2, nucleotide positions 397098 to 494098 found in all three morphotypes.....	111
Table 7. 46-gene deletion from chromosome 2 found in the S1500.....	114

## LIST OF FIGURES

<b>CHAPTER II.</b>	<b>Page</b>
Figure 1. Model of long-term experimental evolution in biofilms.....	21
Figure S1. Biofilm production increases dramatically in B populations.....	27
Figure 2. Adaptive diversification within <i>Burkholderia</i> biofilms.....	28
Figure S2. Images of the smooth or studded (S), ruffled (R), and wrinkly (W) morphotypes from each of six evolved biofilm populations.....	29
Figure 3. Productivity of S, R, and W morphotypes isolated from evolved biofilm populations B1 and B2 grown in monoculture and in mixed communities.....	32
Figure 4. Contributions of cross-feeding and structure to positive effects of biodiversity.....	35
Figure S4. Contributions of cross-feeding and structure to positive effects of biodiversity in population B2.....	37
Figure 5. Absolute and relative effects of cross-feeding in pairwise interactions of supernatant producers and consumers.....	40
Figure 6. Confocal scanning laser microscopy of the evolved biofilm architecture.....	42
 <b>CHAPTER III.</b>	
Figure 1. A. If diversification occurred because of competitive interactions.....	54
Figure 2. Dynamics of morphotype diversity within biofilm population B1 through 1500 generations of experimental evolution.....	59
Figure 3. Relative biofilm fitness values of morphotypes.....	60
Figure 4. Benefits of cross-feeding for all pair-wise interactions.....	62
Figure 5. Dynamics of bead colonization by population B1.....	64
Figure 6. Fitness of the three morphotypes from the Early community.....	66



Figure 7. Absolute fitness of Early genotypes as a function of varying density of another community resident.....69

Figure 8. Relative fitness of Early genotypes.....71

Figure 9. Confocal scanning laser microscopy of the biofilm architecture produced by mutant pairs following 450 generations.....73

**CHAPTER IV.**

Figure 1. Mutational dynamics within a population of *Burkholderia cenocepacia* during 1500 generations of biofilm selection.....87

Figure 2. Selection rate constant of each gene in population B1.....88

Figure 3. Intracellular iron concentrations of each morphotype.....96

## ABSTRACT

### EXPERIMENTAL EVOLUTION OF BURKHOLDERIA CENOCEPACIA BIOFILM POPULATIONS

By

Steffen Ronald Poltak

University of New Hampshire, September, 2010

Many biofilm populations are known for their exceptional biodiversity but the relative contributions of the forces that could promote this diversity are poorly understood. This uncertainty pervades in the well-established communities found on many natural surfaces and in long-term, chronic infections. Here we describe the parallel evolution of cooperative communities derived from a clone of *Burkholderia cenocepacia* during approximately 1500 generations of biofilm selection. This long-term evolution was enabled by a new experimental method that selects for daily cycles of colonization, biofilm assembly, and dispersal. Each of six replicate biofilm populations underwent a common pattern of adaptive morphological diversification, in which three ecologically distinct genotypes arose in the same order of succession and persisted. Mixed communities were more productive than any monoculture and each variant benefited from mixture. These gains in output resulted from asymmetrical cross-feeding between genotypes and the expansion and partitioning of biofilm space that constructed new niches. Furthermore, the diversity found in these was due to unique mutations found in each morphotype detected by complete genome sequencing.

## CHAPTER I

### INTRODUCTION: EXPERIMENTAL EVOLUTION OF MICROBIAL BIOFILM POPULATIONS

#### Chapter I: Introduction

Although most bacteria are readily grown in a nutrient-rich shaking liquid monoculture, it is clear that this is not representative of their experience in nature (Davey and O'Toole 2000; Hall-Stoodley, Costerton et al. 2004). What is more commonly observed is growth in biofilms, where community members reside within secreted polymers of complex carbohydrates, proteins, and occasionally DNA on a biotic or abiotic surface (Hall-Stoodley, Costerton et al. 2004; Thomas, Hiromasa et al. 2009). In contrast to the mass action conditions experienced by planktonic cells, biofilm residents may create spatially structured communities that can be physically and chemically diverse, with varying gradients of nutrients, waste, pH, and oxygen that produce distinct micro-niches for colonization (Stewart and Franklin 2008). Selection of new biofilm immigrants acts on individuals that are most fit in the local conditions even if less fit globally (Ponciano, La et al. 2009). As a result of selection, dynamic biofilm populations often generate more population diversity than planktonic populations in a given period of time (Korona, Nakatsu et al. 1994; Rainey and Travisano 1998; Ponciano, La et al. 2009).

Biofilm populations diversity is commonly observed (Hall-Stoodley, Costerton et al. 2004), yet how selection acts on these populations to

promote diversification is not fully understood (Davies and Geesey 1995; Boles, Thoendel et al. 2004; Brockhurst, Hochberg et al. 2006; Brockhurst, Buckling et al. 2007; Hansen, Rainey et al. 2007; Stewart and Franklin 2008; Xavier, Martinez-Garcia et al. 2009). The challenge in observing adaptation in any system is identifying the environmental factors that influence selection. Fortunately, experimental evolution has empowered our study of the possible causes and consequences of population diversification (Elena and Lenski 2003).

### **A review of experimental evolution in biofilms**

Evolution experiments have been tremendously useful in understanding the dynamics of population ecology and adaptation (Elena and Lenski 2003). In these model systems, researchers capitalize on the two major benefits of microbial models. First, microbial populations reproduce rapidly and produce large populations. Second, microbial species can be readily stored and re-propagated to examine the effects of selection over time. The majority of microbial experimental evolution studies have involved the serial transfer of relatively homogeneous planktonic populations using batch culture or maintaining populations in chemostats for extended periods of time (Elena and Lenski 2003). Additionally, several studies have focused on the influence of spatial structure on the establishment and maintenance of population diversity within a biofilm.

The first study of the effect of spatial structure on population diversity was conducted by Korona et al., in which populations of *E. coli* were grown both on agar surfaces and in well-mixed liquid culture and transferred each day (Korona, Nakatsu et al. 1994). They found that replicate populations grown on an agar surface were more heterogeneous in colony morphology and relative fitness (reproductive rate) than planktonically grown populations. In other studies, Rainey and Travisano demonstrated that populations of *Pseudomonas fluorescens* grown in static broth culture generated new niches, including by forming biofilms at the liquid-air interface (also known as a pellicle), that facilitated the existence of multiple variants (Rainey and Travisano 1998). Boles et al. observed similar diversification of cystic fibrosis (CF) pathogen *Pseudomonas aeruginosa* using flow-cell systems and found that biofilm-derived variants that were able to disperse well from surfaces while others were better biofilm producers (Boles, Thoendel et al. 2004). Finally, Ponciano et al. utilized a flow-cell model to sample isolates at various depths of a mature biofilm and found that isolates from six different depths had unique growth patterns in a variety of media (Ponciano, La et al. 2009). By examining these experiments it is clear that biofilm environments are distinctly different in comparison to planktonic conditions mainly due to their highly structured nature that can promote rapid diversification.

Experimental microbial evolution studies have not only revolutionized our approach to the design of evolution experiments (Korona, Nakatsu et al.

1994; Rainey and Travisano 1998; Ponciano, La et al. 2009), but they have also provided us with valuable insights regarding ecological interactions within the confines of a biofilm. In addition, these studies have begun to clarify (Xavier and Foster 2007; Nadell, Xavier et al. 2009) the adaptive mechanisms that are responsible for the diversification of a biofilm environment (Beaumont, Gallie et al. 2009).

### **Development of a novel model of biofilm experimental evolution: rationale**

Biofilm populations have been studied in nature and under laboratory conditions; however, most biofilm models to date have spanned short time periods. What we have attempted here is to develop a model biofilm evolution model that can be maintained indefinitely with a controlled environment using a single bacterial species that selects for increased biofilm production. In addition, our model allows for daily biofilm disruption through mass action, which is atypical of biofilm experimental populations, especially those grown in flow cells.

The selective environment that we chose was based on one condition found in the human host: a constant temperature of 37°C. We decided to evolve an environmental strain of the bacterial species *Burkholderia cenocepacia* that (as far as we know) had never encountered a human host; however, it is known that environmental strains of this species do frequently

infect the lungs of cystic fibrosis (CF) patients and generate robust biofilm communities. (Coenye, Spilker et al. 2004; Mahenthiralingam, Urban et al. 2005). Ultimately, this system has enabled us to study both the impact of biofilm selective pressures on an adapting bacterial community.

### **Is biofilm diversification driven by competitive or facilitative interactions among community members?**

Members of a biofilm community face an inherent struggle for nutrients and space, which fosters cell-cell interactions that may be competitive or cooperative. Since biofilm cells are essentially fixed within the extracellular polymer, the competition for resources may be exceptionally fierce (Xavier and Foster 2007). Resident members may facilitate the attachment and growth of newcomers by providing a matrix and valuable secondary metabolites. In contrast, existing populations may inhibit the establishment of incoming bacteria. In order to understand the origin of competitive and cooperative interactions it is necessary to identify the environmental factors that could promote them. Since the biofilm matrix connects all community members, the biofilm itself and all the secreted molecules and metabolites contained therein can be considered 'public goods' (Kreft 2004; Brockhurst 2007). These public goods can either harm or benefit individuals and can even be exploited by cheats (Diggle, Griffin et al. 2007; Ross-Gillespie, Gardner et al. 2009). This also includes the bacterial quorum sensing

molecules that allow within and among species communication (Diggle, Griffin et al. 2007).

As a direct result of competitive interactions, new variants may arise that are better adapted to any unoccupied niches generated by resident populations. This facilitative phenomenon is known as niche construction (Odling-Smee, Laland et al. 2003) and has been speculated to be common within biofilm populations (Brockhurst, Hochberg et al. 2006).

### **Biofilm experimental evolution reveals some underlying mechanisms of diversification and adaptation in biofilms**

To date, only a few groups have exhaustively identified the beneficial mutations that occur during the experimental evolution of bacteria (Velicer, Raddatz et al. 2006; Barrick, Yu et al. 2009; Beaumont, Gallie et al. 2009), and no study has identified the mutations accumulated during long-term selection in biofilms. In this study we define the mutations that arose in *Burkholderia* biofilm populations started from a single genotype and passaged for 1500 generations under biofilm selective conditions. Our findings support the hypothesis that selection acts upon genes known to be required for biofilm formation. Additionally, we found significant genetic diversity among distinct lineages and ecotypes arising under biofilm selection, but relatively few genomic lineages were able to persist through 1500 generations. Finally, we propose several potential explanations for the coexistence of multiple lineages.



## **Research goals**

The primary goals of this study were to identify the ecological and evolutionary consequences of bacterial adaptation to a biofilm selective environment. We knew that under planktonic selective conditions that bacterial populations are readily able to evolve to the selective environment (Lenski 1991), but we wanted to see if under biofilm selective conditions the similar adaptation occurred or if the biofilm selective environment was unique. To achieve this goal we identified both the major phenotypic and genotypic changes (if any) that occurred in biofilm and planktonic populations over 1500 generations of serial transfer. We hypothesized that under biofilm selective conditions there would be a greater level of biodiversity maintained due to the structural aspects of biofilm population architecture. Specifically, we aimed to quantify the biofilm production and the effect of population diversity on biofilm productivity. We also predicted that we would find mutations in known genes known to be responsible in biofilm production. Therefore, we aimed to examine the ecological dynamics of biofilm adaptation ultimately identify any underlying adaptive mutations that accumulated in these populations through complete genome sequencing.

## CHAPTER II

### **Ecological succession in long-term experimentally evolved biofilms produces synergistic communities**

#### **Abstract**

Many biofilm populations are known for their exceptional biodiversity but the relative contributions of the forces that could produce this diversity are poorly understood. This uncertainty grows in the old, well-established communities found on many natural surfaces and in long-term, chronic infections. If the prevailing interactions among species within biofilms are positive, productivity should increase with diversity, but if they tend towards competition or antagonism, productivity should decrease. Here we describe the parallel evolution of synergistic communities derived from a clone of *Burkholderia cenocepacia* during approximately 1500 generations of biofilm selection. This long-term evolution was enabled by a new experimental method that selects for daily cycles of colonization, biofilm assembly, and dispersal. Each of six replicate biofilm populations underwent a common pattern of adaptive morphological diversification, in which three ecologically distinct morphotypes arose in the same order of succession and persisted. In two focal populations, mixed communities were more productive than any monoculture and each variant benefited from mixture. These gains in output resulted from asymmetrical cross-feeding between ecotypes and the expansion and partitioning of biofilm space that constructed new niches. Therefore even in the absence of starting genetic variation, prolonged selection for surface

colonization generates a dynamic of ecological succession that enhances productivity.

## **Introduction**

Microbial biofilms may be found on essentially any moist surface, including in soil, on the exterior of larger organisms, or on manmade substrates such as water supply pipes. Though seemingly simple in form and function, the carbohydrate rich matrix that binds unicellular organisms together and affixes them to surfaces can be complex and house varying levels of species diversity. This biodiversity is not lacking for possible explanations, since residents must complete complex life histories from colonization to dispersal and must persist in highly structured environments amongst different competing populations. Neighboring cells can also produce or sequester resources that alter the growth potential of each other and change the local forces of selection, and the biofilm itself can enable variants that might be outcompeted in mass action environments to persist. The net sign of these interactions could either enhance or reduce community productivity and is typically unknown, as is the relationship between biodiversity and productivity in many communities (Cardinale, Wright et al. 2007; Gross and Cardinale 2007). Determining the nature of these interactions can contribute to our understanding of evolution in structured environments in general and of the complexity of biofilm-associated infections in particular.

Despite the basic intuition that diversity is beneficial for biological communities, the forces that generate diversity can span from antagonistic to mutualistic (Hansen, Rainey et al. 2007; Nadell, Xavier et al. 2009; Ponciano, La et al. 2009). Antagonistic interactions could include negative effects of competition, predation (Meyer and Kassen 2007), parasitism (Buckling and Rainey 2002) or social cheating (Rainey and Rainey 2003; Harrison and Buckling 2009) that favor variation but can reduce productivity. The environmental structure of biofilms could also enable diverse populations to coexist that would not persist in mixed, mass-action environments (Rainey and Travisano 1998; Habets, Rozen et al. 2006). Positive interactions among species could include cooperative production of secreted products (Brockhurst 2007), syntrophic metabolic functions (Hansen, Rainey et al. 2007), or the construction of new niches for immigrants by earlier colonists (Odling-Smee, Laland et al. 2003), which should increase productivity.

In theory, the balance of these interactions could change as communities mature over longer periods of time. As examples, the complex microbial communities found in reef ecosystems (Nocker, Lepo et al. 2004), on river bottoms (Lyautey, Jackson et al. 2005), or in sewage pipes (Huang, De Wever et al. 2008) are likely to be many years old and reflect many of the developments in community composition associated with classical ecological succession (Odum 1975; Connell and Slatyer 1977). The same mechanisms that cause species turnover in the plant communities that exemplify succession are also likely to operate in microbial biofilms, with at least the

same level of uncertainty about the relative role of neutral, antagonistic, or facilitative processes (Connell and Slatyer 1977).

Previous studies of experimental evolution in biofilms have occurred over relatively few generations and thus may not reflect the longer-term dynamics occurring in natural populations. We therefore developed a novel long-term experimental model of biofilm selection requiring daily cycles of surface colonization, biofilm assembly, and dispersal. Replicate populations of the bacterium *Burkholderia cenocepacia*, a common resident of the rhizosphere and a pathogen of exceptional concern to the CF community (Ramette, LiPuma et al. 2005), were evolved in this model. We chose a natural isolate from the soil, strain HI2424 (LiPuma, Spilker et al. 2002), as the ancestral clone rather than a clinical isolate because we did not want to limit response to biofilm selection, which likely occurs during colonization of susceptible patients (Costerton 2001). In a previous study we found that this same strain was capable of rapid adaptation to laboratory conditions distinct from those described here, with consequences for host specificity (Ellis and Cooper 2010). In this study, we predicted that adaptation would also be accompanied by diversification because of the structure and greater complexity of the biofilm environment.

Our initial objectives were to quantify the fitness of various evolved clones in monoculture and when assembled in the mixed community and to identify the ecological forces favoring any variation. Bacterial species like *Burkholderia* and *Pseudomonas* that infect the lungs of cystic fibrosis (CF) patients often exhibit heritable variability in biofilm phenotypes following

selection in the host lung (Singh, Schaefer et al. 2000; Haussler, Lehmann et al. 2003; Nguyen and Singh 2006; Smith, Buckley et al. 2006), which may reflect adaptation to distinct conditions within the host. Although the contributions of each bacterial variant to the biofilm community are uncertain, some morphotypes have been associated with increased mortality (Haussler, Lehmann et al. 2003; Chantratita, Wuthiekanun et al. 2007; Starkey, Hickman et al. 2009). Understanding how diversity influences the productivity of these infections and their consequent resilience and pathogenicity is therefore a high priority.

Following approximately 1500 generations of experimental evolution favoring cycles of surface colonization, biofilm construction, and dispersal, we found that diversity, characterized by colony morphology, growth dynamics, and region of growth in the biofilm, evolved in each of six replicate populations. The three variants that evolved in each population appear similar to the variants in other populations, became detectable in the same order, and were associated with increased cellular productivity. Further, we found that diversity was maintained by ecotypes that improve both space and resource availability in the selective environment.

## **Materials and Methods**

### **Experimental evolution**

We devised a novel method of studying biofilm evolution by transferring biofilm associated cells that adhered to a 7mm plastic bead

floating in a 15x180mm test tube rotating in a rollerdrum at 50rpm (Fig. 1). Each day, a new bead was colonized and a new biofilm constructed, selecting for a regular cycle of colonization and dispersal. Cells that adhered to the tube walls or remained in planktonic culture were not transferred. Six replicate biofilm populations (B populations) and six control, planktonic populations (P populations) were each founded by a single HI2424 clone and grown in 5ml M9 minimal medium with 1M galactose, a major constituent of mucus that promotes biofilm formation. Populations were serially transferred every 24 hours for 143 days at 37°C on a rollerdrum at 50 rpm. At the start of the experiment, B population transfers into fresh media produced dilutions of  $\sim 1.5 \times 10^3$ , but this dilution declined over time to  $\sim 1.0 \times 10^3$  owing to increased numbers of cells adhering to the bead. The number of generations is  $143 \cdot \log_2(\text{dilution})$ , so we infer that between 1425 and 1509 generations occurred in B populations and 1000 generations occurred in P populations.

Figure 1

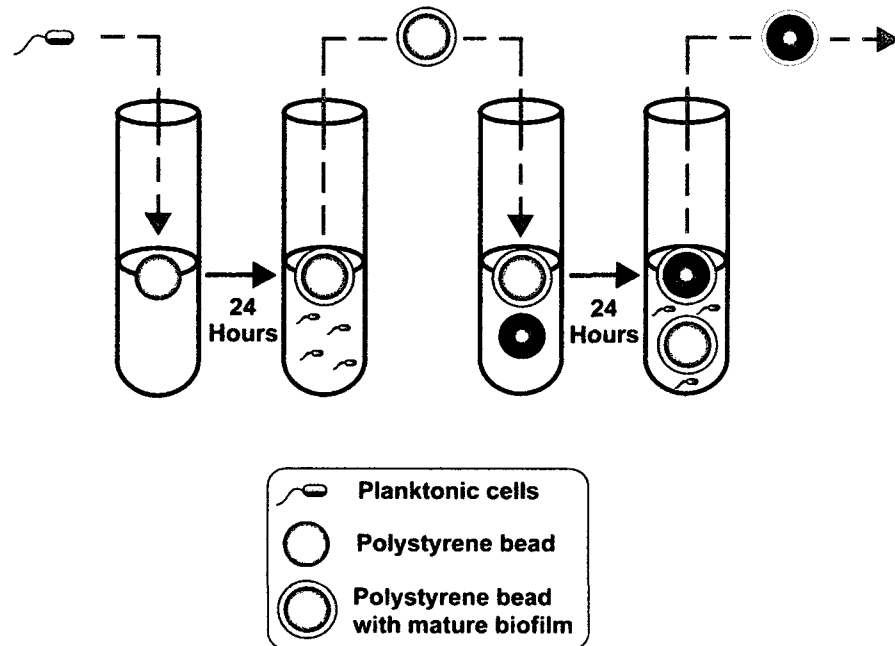


Figure 1. Model of long-term experimental evolution in biofilms. Six replicate populations founded with a single clone of *B. cenocepacia* HI2424 were propagated on 7mm polystyrene beads suspended in 5ml M9 + 1M galactose and were sterilely transferred to new media every 24 hours. Each bead population was required to colonize a new oppositely marked bead each day. Control, planktonic populations were serially transferred via 1:100 dilutions of planktonic cells grown in 5ml M9 + 1M galactose for 24 hours (not shown).



This model of biofilm selection differs from previous methods relying on static culture (Rainey and Travisano 1998) or flow cells (Boles, Thoendel et al. 2004) in that: i) a new biofilm must grow on an uncolonized surface each day; ii) the biofilm is subject to frequent shear forces in the rotating tube, and iii) samples of evolving populations can be archived and reconstituted under identical experimental conditions. In addition, our experimental model incorporates a variety of bacterial life-history components that can be separately quantified, namely dispersal, planktonic growth, and surface recolonization.

### **Genetic manipulations**

A LacZ<sup>+</sup> mutant of *B. cenocepacia* was generated by insertion of pCELacZ (Ellis and Cooper 2010), which inserts *lacZ* and *dhfr* in specific sites by Tn7. Transposants were competed against a *dhfr*-marked strain of HI2424 in several types of media and no fitness effect of the *lacZ* insertion was observed. Plasmids pSPR (red) and pSPY (yellow) were constructed using by inserting genes encoding fluorescent proteins into pBBR1MCS, which encodes chloramphenicol (Cm) resistance (Kovach, Elzer et al. 1995). pSPR harbors the red fluorescent protein gene from DsRedExpress (Lambertsen, Sternberg et al. 2004) and pSPY the EYFP gene (Lambertsen, Sternberg et al. 2004), both bounded by KpnI-XmaI restriction sites that are also found in pBBR1MCS. Plasmids were introduced into evolved morphotypes by electroporation and positive selection at Tryptic-Soy Agar + 150 mg/ml Cm.

### **Morphotype identification**

Colony variants were scored following growth on T-Soy agar plates for 24 h at 37°C and then 48 h at room temperature. Variation in colony morphology within biofilm populations was evident following plating at generation 150; morphotype heritability was confirmed by continued isolated passage on plates and in both planktonic and biofilm environments.

### **Productivity assays**

Biofilm productivity was quantified as CFU/ml from beads colonized during 24 h in the selective environment by vortexing beads in 1.5ml PBS for 1.5 min. To verify the effectiveness of vortexing for removing biofilms from beads, we examined vortexed beads under scanning electron microscopy using standard methods and found very few remaining adherent cells (at least 1000-fold reduction per unit area). Moreover, plate counts were consistent among replicates and with the optical density of the medium, which suggests that colonies were not founded by clumps, whose size should be random. Planktonic yield was measured as CFU/ml from the planktonic fraction of tubes lacking beads, without sampling wall growth. Total biomass of clones and the mixed community from population B1 was quantified with fivefold replication as follows. Cultures were grown from freezer stock in tubes containing 4ml M9+galactose and 1ml LB and then subcultured into tubes containing 5ml M9 + galactose and a 7mm bead. The mass of each bead was measured prior to the experiment. Following 24h of incubation under the selective conditions, beads were removed from each replicate, placed in separate wells of a 24-well plate, and dried at 80 C for 30 min. The mass of

each bead was subsequently measured and dry-weight biomass was inferred from the difference from the original uncultured bead.

### **Fitness assays**

Fitness was measured as  $\ln(N_{t=24}/N_{t=0})$  in both environments beginning with resuspended planktonic cells or vortexed biofilms. When calculating expected productivity based on yields of each mutant in monoculture, as in Figures 2, 3, and S3, calculating standard confidence intervals of expected productivity was impossible as these were separate experiments. However, simulated 95% confidence intervals based on arbitrary pairings of measures from each monoculture replicate were  $< 0.2\%$  of the expected mean. Biofilm production was measured by crystal violet staining (O'Toole, Pratt et al. 1999) in 96 well plates (Corning Costar) following 24 h of incubation with shaking at 37°C and 150 rpm.

To examine the dynamics of attachment to the bead over the growth cycle, a single mixed culture of population B1 grown overnight under selective conditions was used to inoculate 18 fresh tubes containing beads, each grown under selective conditions. Beads from three replicate cultures were destructively sampled after 4, 8, 12, 17, 20, and 24 hours, by vortexing in 1.5 ml of PBS, dilution and plating on tryptic soy (7g/L) agar to obtain CFU/ml and morphotype frequencies at each time point.

### **Effects of environmental structure on biodiversity**

We added an additional polystyrene bead (more structure) or removed the bead (no structure) from cultures of populations B1 and B2 grown under conditions that were otherwise identical to the selective regime. The variation in colony morphology (or biodiversity) of >200 colonies from each treatment was measured using the Shannon-Wiener index:  $H = -\sum(P_i \log[P_i])$ , where  $P_i$  = the proportion of each given subspecies in the population.

### **Cross-feeding assays**

Following 24 h of growth in the selective environment, cells were pelleted by centrifugation and the supernatant passed through a 0.22mm filter. Samples (200µl) of each supernatant were added to 96 well polystyrene plates (Corning), and each morphotype was inoculated with  $10^6$  CFU and incubated at 37°C for 24 h, recording optical density (OD600) following shaking every 15 min. Growth in supernatant was compared to a concurrent assay of growth in the unaltered evolution medium and expressed relative to these measures.

### **Microscopy**

Morphotypes containing either pSPR or pSPY were grown individually on beads under standard selective conditions supplemented with 50mg/ml chloramphenicol to maintain positive plasmid selection. Cultures were sub-cultured from beads into selective media containing 1cm X 1cm polystyrene slides. Each culture was induced with 30ml of 10mM IPTG for 12 hours before imaging. To label the third morphotype that was unmarked by a

plasmid, slides were stained with TOPRO-3 (Invitrogen), which stains DNA, for 1 hour and destained in PBS for 15 min. Slides were cleaned with ethanol on one side and placed on 75 X 25 mm glass slide (Corning). DABCO (Sigma) (25mg/ml) in glycerol (0.3ml) was added to the biofilm side and a 1.5 in. glass cover slip was placed on top. Images were captured at 200X and 400X magnification using 2048 dpi. The following excitation and emission settings were used for each marker: pSPY: 514nm/527nm, pSPR: 556/586, TOPRO-3, 633/651. Z-stack images spanned from top to bottom of biofilm. Further image analysis was conducted using Carl Zeiss Zen Light Edition® software.

## **Results**

### **Biofilm populations undergo successive adaptive diversification**

As expected, biofilm production increased in all B populations but only marginally in control P populations (Fig. S1). In addition, all six B populations diversified into three classes of heritable colony morphologies (morphotypes) distinct from the ancestor, termed smooth or studded (S), ruffled spreader (R), and wrinkly (W) (population B1: Fig. 2, populations B1-B6: Fig. S2). In each population, an S variant (with greater opacity, more defined colony boundaries, and increased uptake of Congo Red dye) was detected, often in the majority, in the first sample at 150 generations. At the following sample at 300 generations, we detected an R variant (with rough or rugose texture and greater size) and then between 300 and 450 generations, a W variant (small, dense, highly rugose, and the greatest biofilm producers). Although the

morphologies of these mutant colonies varied among replicate evolved populations, they nevertheless are readily distinguishable as common types (Fig. S2) that inhabit similar regions of the test tube (as in Fig. 1).

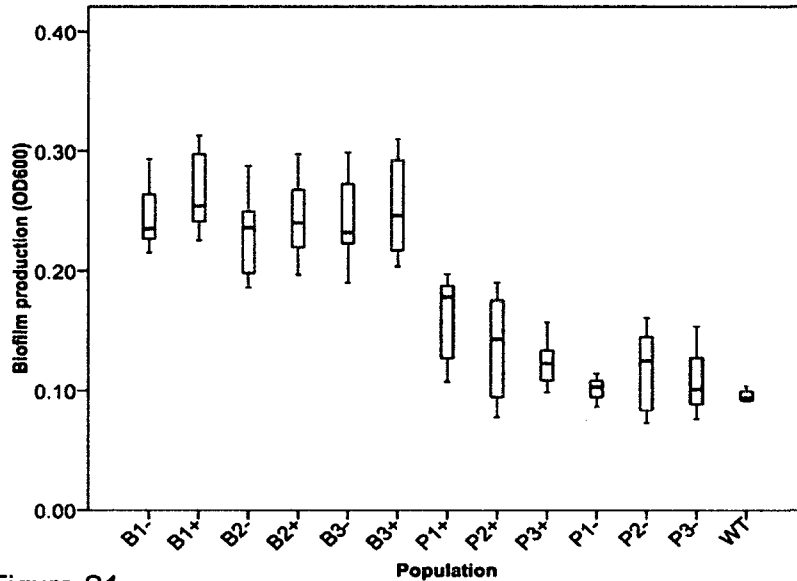


Figure S1

Figure S1. Biofilm production increases dramatically in B populations and only marginally in P populations, following 1500 generations of biofilm selection or 1000 generations of planktonic selection, respectively. Boxplots illustrate mean, upper and lower quartiles, and 95% confidence intervals of each population, based on three clones measured in triplicate. B clones are one each of randomly selected S, R, and W morphs; P clones were randomly chosen as they were monomorphic. Biofilm readings are unusually low owing to an experiment-wide staining effect but rankings are consistent among experimental blocks.

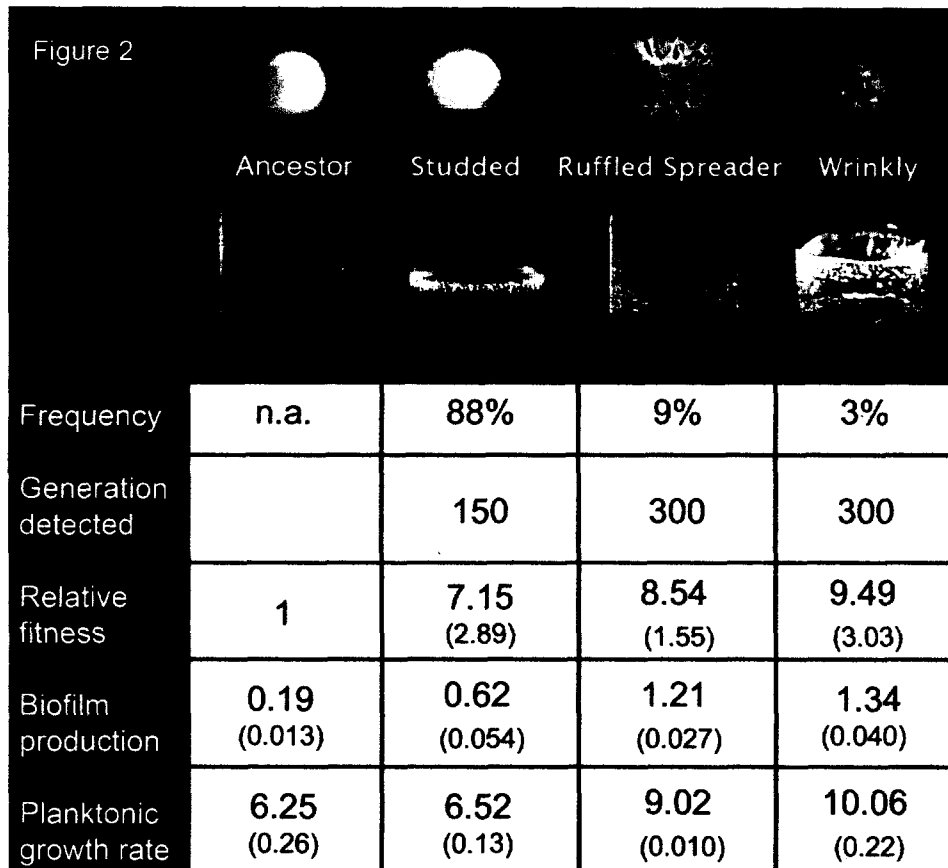


Figure 2. Adaptive diversification within *Burkholderia* biofilms. Colony morphologies (first row) and biofilm phenotypes (second row, growth on tube walls) of genotypes following ~1,500 generations of biofilm selection, their timing of detection in population B1, and their associated phenotypes. All six biofilm-evolved populations produced morphologically similar genotypes (Studded = S, Ruffled Spreader = R, Wrinkly = W, Fig. S2) that were detected during the same intervals. Morphotypes differ in their fitness, colonization patterns, growth rates, and biofilm production when grown in monoculture. Relative fitness is colonization efficiency of evolved genotypes relative to the ancestor. Planktonic doubling time (increasing values being disadvantageous)

and biofilm production were measured using standard techniques. 95% confidence intervals of each measurement are in parentheses.

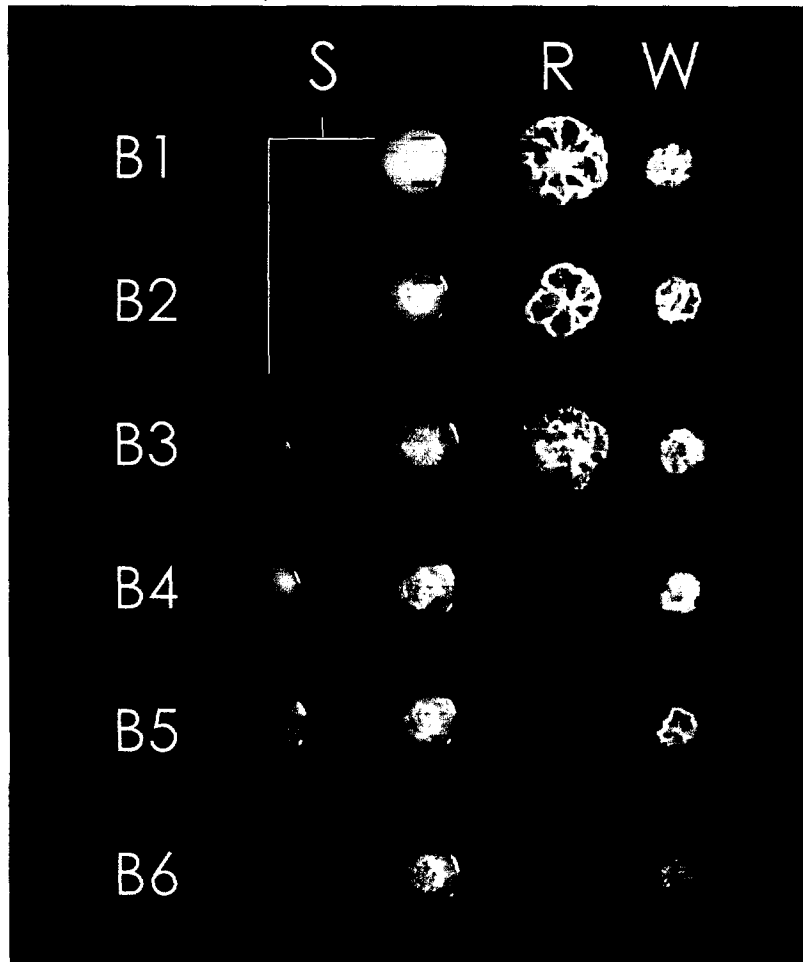


Figure S2. Images of the smooth or studded (S), ruffled (R), and wrinkly (W) morphotypes from each of six evolved biofilm populations. Homogeneity among morphotypes from different populations and their common times of origin (S at 150 generations, R at 300 generations, and W at 300-450 generations) suggests adaptation to common conditions.



Focusing on the clones isolated from population B1, each biofilm morphotype greatly outcompetes the ancestor in the selective environment, produces different levels of biofilm in monoculture with concomitant reduced planktonic growth rates, grows in different regions of the tube when in monoculture, and persisted over nearly five months of transfer (Fig. 2). In contrast, only one P population gave rise to a new colony type similar to S, suggesting that selection in the structured biofilm environment favors morphological and functional diversification. Indeed, eliminating structure from two of these populations at 1500 generations by removing the bead significantly reduced diversity after 24 hours (Shannon-Wiener  $H$ ; population B1,  $t = 16.30$ ,  $df = 4$ ,  $p < 0.0001$ ; population B2:  $t = 385.4$ ,  $df = 4$ ,  $p < 10^{-9}$ ). Based on the rapid decline in abundance of R and W, only S is expected to persist during prolonged transfer, and hence the stability of biofilm diversity depends on its structure.

### **Mixed populations are more productive because of complementary interactions**

We measured effects of diversity on productivity in the selective environment by comparing the viable cell yield of two evolved mixed biofilm communities with those of their constituent morphotypes when grown alone. The cellular productivity of both mixed populations was much greater than any of their constituents in monoculture ( $p < 10^{-5}$  in all t-tests, Fig. 3), and in both populations the S variant attained higher yield in the mixture than in monoculture (B1:  $t = 47.1$ ,  $df = 6$ ,  $p < 10^{-8}$ , B2:  $t = 32.3$ ,  $df = 6$ ,  $p < 10^{-8}$ ). This synergy did not appear to be the product of hidden diversity in the mixed

sample because populations of single clones of S, R, and W grown at frequencies approximating those of the mixed sample reproduced the attributes of the complete mixed community ( $t = 0.53$ ,  $df = 8$ ,  $p = 0.61$ ). However, this increase in cellular productivity did not equate to increased dry-weight biomass of the mixed community. Morphotypes and the mixed community varied significantly in biomass production ( $F_{15,4} = 17.1$ ,  $p < 0.001$ ) but the high-biofilm variants R and W were most productive in this assay, in the following rank order (W,R) > (S, Mixed) > WT (based on Tukey-Kramer post-hoc tests). Given that the mixed community is >85% S, it is not surprising that its biomass is indistinguishable from that of S; further, R and W clearly produce more exopolysaccharide (Fig. 1) than S.

Biodiversity may lead to increased cellular productivity of the community by two general processes: selection and complementarity (Loreau and Hector 2001). Selection refers to “overyielding” of the types that are most productive in monoculture, typically because they are better competitors. In contrast, complementarity reflects positive effects of biodiversity on most or all community members, either by resource partitioning or facilitation between species (Loreau and Hector 2001). We distinguished the contributions of selection and complementarity to biofilm productivity using established methods (Price 1970; Loreau and Hector 2001) that test whether mixed communities depart from additive expectations of the growth of each component species, given known starting frequencies and productivity in monoculture.

Figure 3

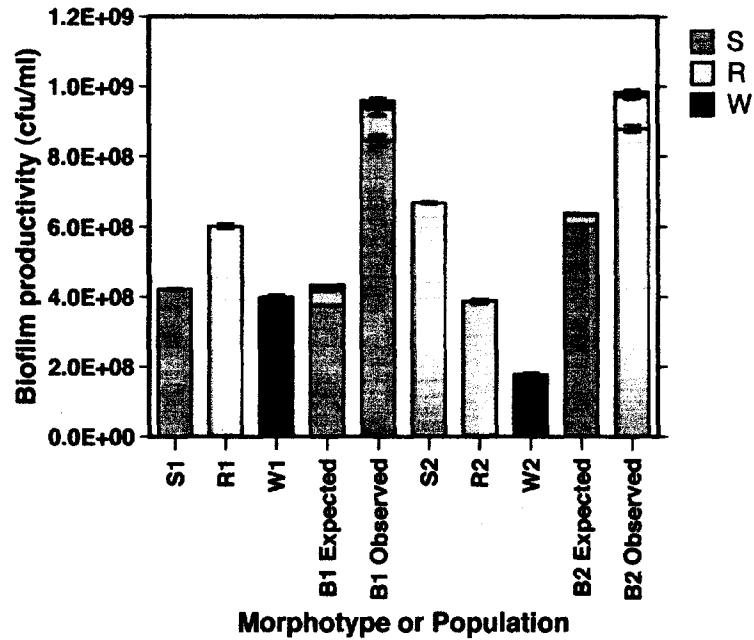


Figure 3. Productivity of S, R, and W morphotypes isolated from evolved biofilm populations B1 and B2 grown in monoculture and in mixed communities. Expected productivity was calculated as the product of the proportion of each morphotype in the founding population and its yield (CFU/ml) in monoculture (Loreau and Hector 2001). Observed productivity is the total yield of the mixed community in the experimental environment. Error bars are 95% c.i. based on four replicates.

Consistent with an effect of selection, the S type remained numerically dominant in both populations, but its proportion of the total community actually decreased slightly in both mixed populations as the rarer R and W variants increased from their low starting frequencies, which better reflects complementarity. Although the R and W types that produce more biofilm do not grow as well as they do in monoculture, presumably because of their slower growth rates and inferiority in competing against S for nutrients (Fig. 2), they are nevertheless more productive than expected when competing in mixed culture. In population B1, the productivity of S increased by 2.25-fold, R by 2.21-fold, and W by 1.36-fold, resulting in 109% complementarity and -9% selection. In population B2, the productivity of S increased by 1.45-fold, R by 3.18-fold and W by 3.91-fold, resulting in 75% complementarity and 25% selection (Fig. 3). Each ecotype thus benefits greatly from growth in the mixed community, causing the total populations to more than double in size due to the dominant facilitative effect of complementarity.

### **Spatial partitioning and cross-feeding generate community synergy**

We focused on two potential causes of increased productivity in the focal B1 and B2 populations: more efficient use of space by diverse types and more efficient use of available nutrients (e.g. cross-feeding (Rozen, Nadège et al. 2009)). Partitioning of space could underlie community synergy if growth of biofilm engineers increased the total surface area for attachment and growth of all variants. Likewise, secondary metabolites could facilitate growth of other variants if they are more efficient or productive on these resources than their producers. To isolate the independent contributions of space and

cross-feeding to the observed gain in productivity, we measured yields of monocultures and mixed populations in environments either lacking the bead, which eliminates structure and isolates the potential effects of cross-feeding, or containing two beads, which doubles the potential surface for adherence. In both tests, as in the long-term selection, growth on the tube walls was not sampled. Mixed populations were more productive than expected in all environments (Fig. 4, Fig. S3), which demonstrates that both mechanisms operate, but S, R, and W each benefit from different combinations of space and cross-feeding. Specifically, by removing the bead to emphasize cross-feeding, only S significantly benefits from growing in the mixed community ( $t = 14.3$ ,  $df = 8$ ,  $p < 0.001$ ) and R and W decline in frequency (Figure 4B). In contrast, by adding a bead to double the available space, the productivity of R and W increase in the mixed community (R:  $t = 16.4$ ,  $df = 6$ ,  $p < 0.001$ ; W:  $t = 55.6$ ,  $df = 6$ ,  $p < 0.001$ ) and the yield of S actually declines slightly ( $t = 3.62$ ,  $df = 6$ ,  $p = 0.011$ ). Mixed populations of B1 and B2 differed in their responses to varying environmental structure: in B1, the greatest advantage of diversity was found in the single-bead environment (Fig. 4B) but in B2 the greatest transient advantage of diversity was found without the bead as S overgrew the mixture (Fig. S3B). These distinct responses to altered environmental structure demonstrate that the mechanisms that maintain diversity differ between populations, perhaps as a consequence of unique adaptive paths or different coevolutionary dynamics among the morphotypes.

Figure 4

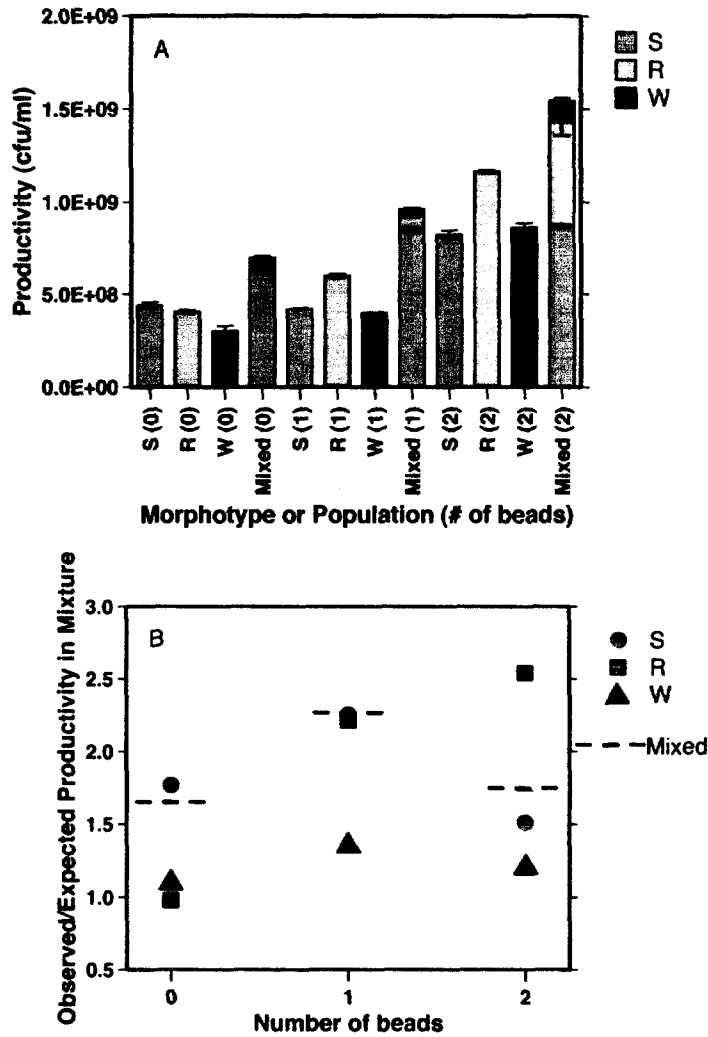


Figure 4. Contributions of cross-feeding and structure to positive effects of biodiversity. Morphotypes from population B1 were grown either in monoculture or in mixed communities in environments containing no bead (cross-feeding only), 1 bead (cross-feeding + structure), or 2 beads (cross-feeding + 2X structure). A. Productivity (CFU/ml) and diversity are greatest in the most structured, 2-bead environment but productivity benefits from

diversity in all environments. Error bars are 95% c.i. based on four replicates.

B. Relative effect of biodiversity (observed/expected productivity) for each morphotype in the mixed communities (symbols in legend) and the overall effect on the mixed community itself (dashed line); expected yield was calculated as described (Loreau and Hector 2001). Effects of biodiversity are greatest in the 1-bead environment in which selection occurred.

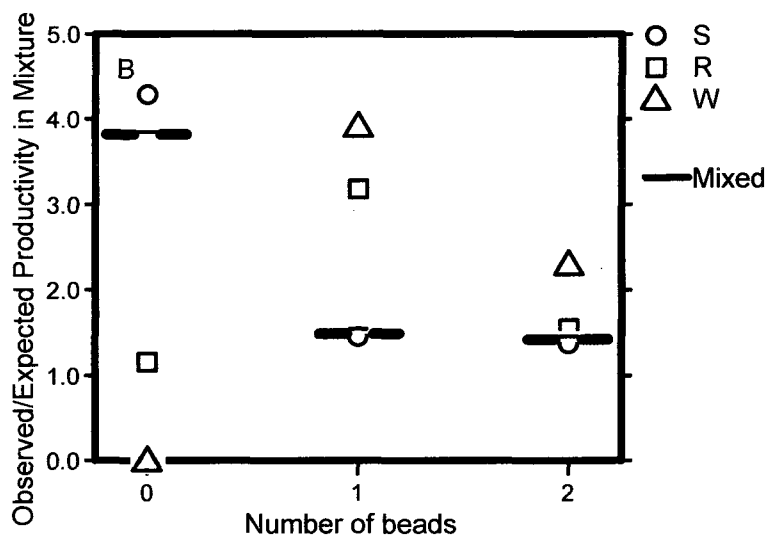
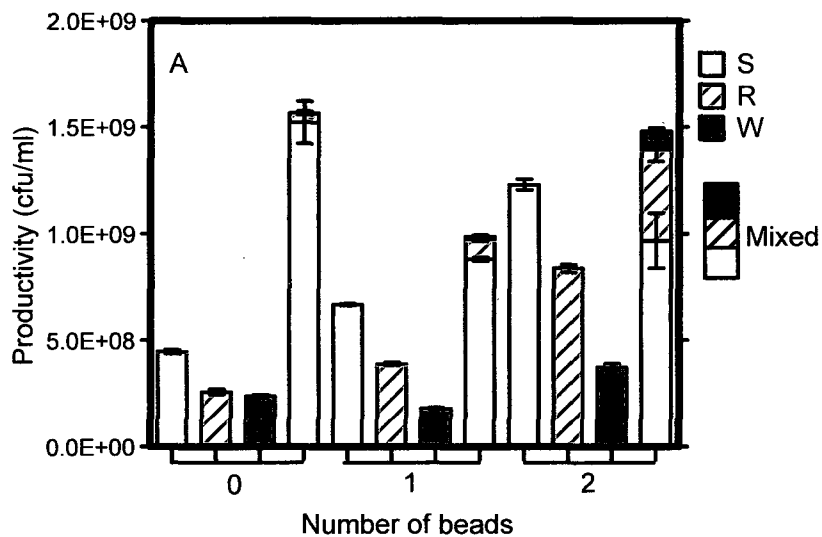


Figure S4. Contributions of cross-feeding and structure to positive effects of biodiversity in population B2. Morphotypes were grown either in monoculture or in mixed communities in environments containing no bead (cross-feeding only), 1 bead (cross-feeding + structure), or 2 beads (cross-feeding + 2X structure). A. Productivity (CFU/ml) is greatest in the 0-bead environment



owing to overyielding of the S variant but is greater than expected in the mixed community in all environments. The most structured 2-bead environment is the most diverse; the W variant was undetectable in the mixed community grown without a bead. Error bars are 95% c.i based on four replicates. B. Relative effect of biodiversity (observed/expected productivity) for each morphotype in the mixed communities (symbols in legend) and the overall effect on the mixed community itself (dashed line); expected yield was calculated as described (27). S benefits from diversity due to cross-feeding and perhaps because consumer variants R and W decline in frequency (0 beads) whereas R and W benefit from spatial partitioning (1 or 2 beads).

To better quantify effects of cross-feeding we grew isolates of S, R, and W from population B1 in their own cell-free supernatant and in the supernatant of all other morphotypes plus the ancestor. Remarkably, all morphotypes grew better in supernatant than in the original medium (Table S1), although we acknowledge that these assays were conducted under conditions different from the selection environment. However, morphotypes varied in the extent to which they improved the growth medium and these benefits were asymmetrical (Fig. 5). Specifically, S grew best in its own supernatant, increasing its own productivity more than 5-fold over growth in unconditioned medium (Fig. 5B), but it also grew better than the other variants in their supernatants (Fig. 5A). These results demonstrate why S remains at high frequency under all conditions. In contrast, the R variant grew best in the supernatant of the mixed community, the W variant grew best in

either the supernatants of S or R, and neither R nor W could grow in their own supernatants. Thus both R and W benefit greatly from the metabolic by-products of other community members but not their own, producing a strongly interdependent food web in which only S is self-sustaining. Surprisingly, the rarest W type was essentially unable to grow in the supernatant extracted from the mixed community (Fig. 5C), which may be caused by self-inhibition or by the other morphotypes depleting nutrients below usable levels. For W to grow on the metabolites of S or R in a mixed community, local and structured producer-consumer interactions may be required.

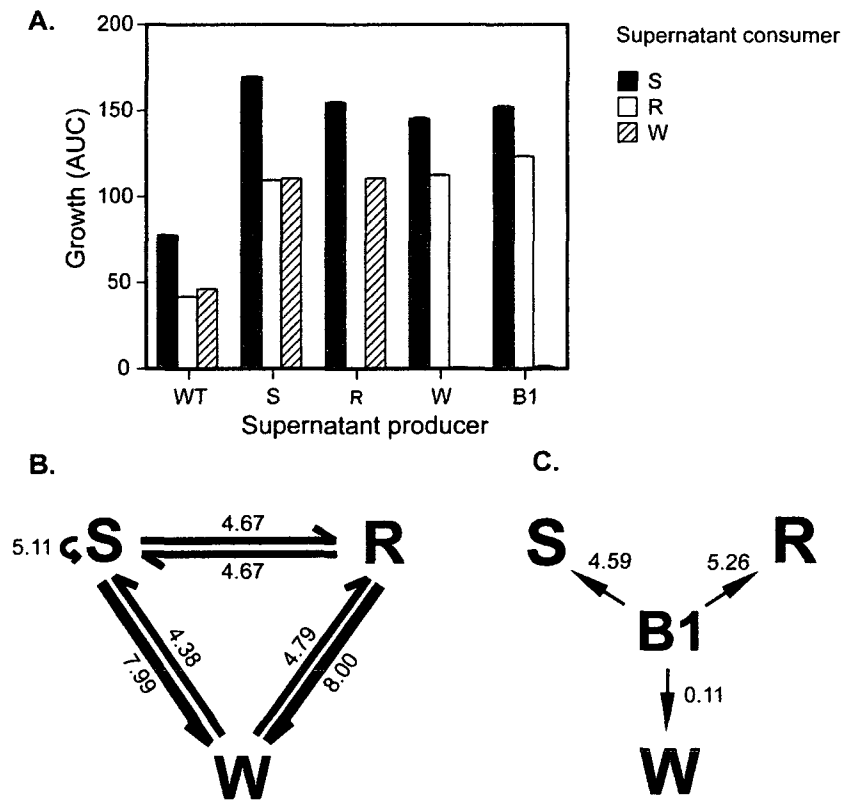


Figure 5. Absolute and relative effects of cross-feeding in pairwise interactions of supernatant producers and consumers. Isolates from population B1 and the ancestor (Jones C.G.) were grown in the cell-free supernatant produced by themselves and each other type.. A. Growth (measured as the area under the curve of OD600 over 24h,  $\pm$  95% ci, n=5) of each genotype in supernatants produced by fellow community genotypes. B. Cross-feeding interactions between genotypes. Numerical values indicate fold-increase in supernatant growth relative to growth in unconditioned

medium. C. Effects of growth by each genotype in the supernatant of the mixed community of population B1, calculated as in part B.

**Biofilm population architecture.** To explore how the variants partitioned biofilm space, we imaged a mixed community of fluorescently labeled S, R, and W from population B1 using confocal laser scanning microscopy (CLSM, Fig. 6). These images indicate that each morphotype adheres and contributes to biofilm assembly in a distinct pattern. Specifically, S cells tend to carpet the biotic surface of the biofilm (Fig. 6A); R cells adhere to the plastic surface more effectively but spread rather than grow vertically (Fig. 5B), and W cells produce the tallest and densest aggregates (Fig 5C). R and W variants are clearly segregated as distinct clusters across the surface, whereas S mostly inhabits a unique surface layer of the Z dimension and is more diffuse. The purple color in the assembled biofilm (Fig. 6C) demonstrates a specific association between S (blue) and W (red) cells. The finding that W cells are rarely found without S may result from cross-feeding that benefits W and structural synergy that benefits S. Furthermore, the depth of the biofilm generally reaches its maximum only when all three variants are present: removing any one variant produces a biofilm with less surface coverage, height, and structural resilience to physical disruption.

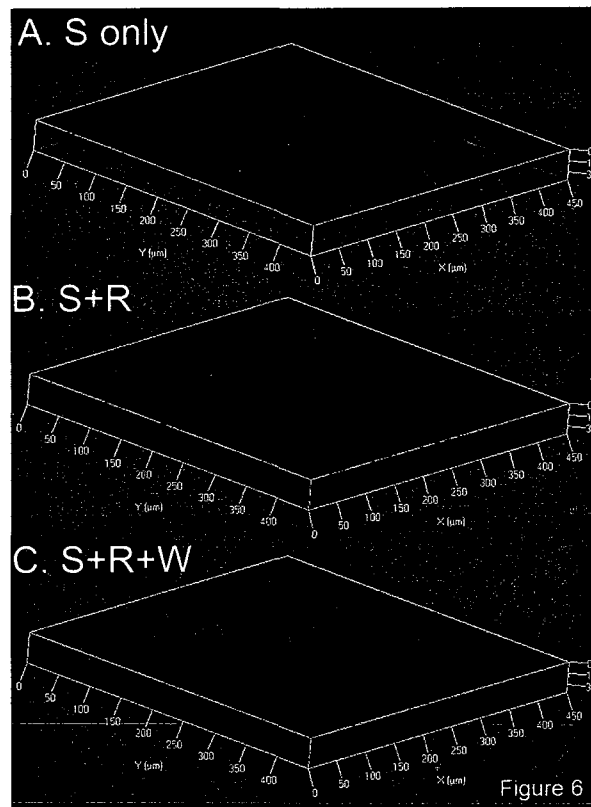


Figure 6. Confocal scanning laser microscopy of the evolved biofilm architecture. The biofilm produced by population B1 after 24h on a polystyrene slide was rendered in three dimensions. The entire biofilm was stained with TOPRO-3 (Invitrogen) and is projected in blue, the W genotype carries pSPR and fluoresces red, and the R genotype carries pSPY and is projected in green. Each morphotype inhabits a different region, and S builds clusters atop the R (indicated by yellow) and especially the W morphotype (indicated by purple).

This biofilm architecture, in which the type that grows best (S) is found more on the biofilm exterior than on the plastic surface, led us to examine the timing of attachment of each type during the growth cycle, as the biofilm specialists R and W would be expected to attach first. Replicate cultures of the mixed population B1 were grown in the selective environment and beads were destructively sampled at regular intervals over 24 hours to examine their biofilm composition. As expected, W, which sticks most strongly to the bead (and tube walls) in monoculture, is the earliest colonist and reaches a frequency of 25% between four and six hours. Its frequency then begins to decline as R increases in frequency, reaching its maximum at 18 hours. The density and ultimately the frequency of S rises steadily throughout the growth cycle, reaching >85% by 24 hours (Fig. 2). The daily assembly of the biofilm on the bead is therefore ordered in a pattern of succession that is opposite of when the ecotypes became detectable during evolution: the early evolved S attaches to the later evolved R and W, which are better surface colonists.

## **Discussion**

Diversity is a defining trait of the biofilm lifestyle but the relative contributions of factors promoting diversity have been unclear. Biofilms are inherently structured (and slimy or sticky) environments, and this structure alone could maintain diversity that would otherwise be eliminated by competition in more uniform environments. However, the exceptional

biodiversity of some microbial surface communities (>700 species may be identified in dental plaque (Kuramitsu, He et al. 2007) suggests that it is the interactions between species – perhaps facilitated by environmental structure – that generate biodiversity. These interactions can span from antagonistic to mutualistic and influence community dynamics and productivity in unpredictable ways, particularly as biodiversity accumulates over longer periods of time.

To study the evolutionary consequences of prolonged biofilm selection and the ecological dynamics and forces that could contribute to biofilm diversity, we devised a novel model of biofilm selection and studied adaptation and diversification in six replicate biofilm populations of *B. cenocepacia*. As a control, six replicate populations were simultaneously transferred under conditions favoring planktonic growth under the same nutrient conditions.

Not unexpectedly, we found that heritable diversity, based on colony morphology, evolved in biofilm populations but was not detected in evolved planktonic populations. However, more surprising was that novel colony types arose in a common pattern of succession in all six populations: S, then R, then W. When grown separately, these morphotypes grow in separate regions of the test tube that suggest spatial specificity of their biofilms, but when grown together, the mixed community is more productive than any one type grown alone (Fig. 3). To understand the basis of this synergy we modified the environment by increasing or decreasing the available space and thus the relative role of cross-feeding. When the plastic bead was

removed, only S significantly benefited from growing in the mixed community whereas R and W declined in number (Fig. 4). In contrast, when a second bead was added, the frequency of R and W increased in the mixed community and the yield of S was unaffected. Therefore, in spite of their ability to feed on S metabolites, R and W require surface binding to persist (and benefit from increased surface area) but S can sustain itself at a lower productivity level in the absence of R and W.

Although morphotypes appeared at similar times in replicate biofilm populations and functioned similarly in monoculture, not every population responded equally when environmental structure was altered. In B1, the greatest advantage of diversity was found in the single-bead environment (Fig. 4B) but in B2 the S morphotype grew much better than expected when the bead was removed (Fig. S3B) and the W morphotype became undetectable. These findings demonstrate that the ecological mechanisms that maintain biodiversity vary among populations as products of distinct adaptive mechanisms, forms of niche partitioning, and/or coevolution among types. Close inspection of the colony morphologies and correlated phenotypes of the S, R, and W mutants from replicate populations (Fig. S2) suggests that they likely represent distinct adaptations with similar ecological consequences, but whether these different ecotypes are genetically and functionally equivalent is unknown and a subject of ongoing study.

Although this report focuses primarily on the ecological mechanisms that maintain biofilm biodiversity, we can infer how these variants initially rose to high frequency. S likely arose first because it could better exploit the



selective environment than its ancestor, primarily as a better competitor for the medium but also by producing more biofilm (Fig. 2, Fig. 5). Yet during each cycle, S colonizes the new bead surface relatively late after growing best among the variants in the medium and secreting metabolites for later use. R and W may have evolved in response by exploiting the vacant bead surface and specifically consuming these metabolites (Fig. 5B). Although both R and especially W remain at low frequency because of their slow growth rates (Fig. 2) and because of their lesser final productivity (Fig. 5A), their greatly increased biofilm production facilitate much greater attachment of S (Figs. 3 and 6) and each other to the polystyrene bead. Such dynamics may therefore be viewed as one of succession enabled by niche construction (Odling-Smee, Laland et al. 2003), although it is plausible that the initial invasions by biofilm specialists were driven by competition or tolerance more than facilitation (Connell and Slatyer 1977; Day and Young 2004).

Odum (1963) pointed out that the well-recognized phenomenon of ecological succession can be propelled by the processes of community residents themselves, including their evolved progeny, or by changing external abiotic conditions (Odum 1975). He then defined three parameters of succession that we suggest describe the dynamics of these biofilm communities well: 1) it is orderly, reasonably directional, and predictable; 2) it results from the modification of the environment by the community, and 3) it maximizes productivity and stability (Odum 1975). The parallel, sequential rise of three distinct morphotypes in each population (Fig. 2, Fig. S2) fulfills the first parameter, and the increased biofilm (Fig. 2, Fig. 6) and production of

novel metabolites for cross-feeding (Fig. 5) fulfill the second. The third outcome of maximum productivity and stability is least certain, though we point out that these morphotypes coexisted in all replicate populations for more than 1,000 generations after their origin, with obvious increases in cellular productivity and surface coverage (Fig. 6). Finally, because all diversity arose from a single ancestral clone in constant abiotic conditions, these populations highlight the need to consider evolutionary processes as well as strictly ecological ones in the development of ecosystems (Odum 1975).

Our experimental method enabled biofilm selection for five months but could theoretically proceed indefinitely and mimic the scale of prolonged chronic infections or more beneficial host associations. This is also one of the first experimental evolution projects with *Burkholderia*, a genus whose functional diversity and tendency to associate with a wide range of hosts with varying consequences demands further study (Parke and Gurian-Sherman 2001; Ellis and Cooper 2010). *Burkholderia* species are found in many biofilm associated environments and their infections are associated with biofilms, either as sources of contamination or as responses to antimicrobials. We note that the colony morphologies that evolved in each experimental population have been widely reported as associated with chronic *Burkholderia* and *Pseudomonas* infections with increased virulence and, like these experimentally evolved types, produce much greater biofilm in laboratory culture (Haussler, Lehmann et al. 2003; Chantratita, Wuthiekanun et al. 2007; Starkey, Hickman et al. 2009) (see Chantratita et al. 2007, Fig. 2 in

particular). A forthcoming study will compare the genetic bases of these experimental variants with those isolated from biofilm-associated infections of persons with CF to test whether the similar colony morphologies are caused by parallel molecular adaptations. More practically, we suggest that our model may enable manipulative experiments *in vitro* that could shed light on the patterns of succession and concomitant increased resilience of chronic biofilm-related infections (Rakhimova, Munder et al. 2008).

This system also enables further mechanistic study of the evolution and maintenance of diverse communities. The relationship between diversity and productivity has remained uncertain because of the multitude of potential interactions in complex communities; for example, a positive correlation need not exist if diversification occurs by the evolution of cheats (Rainey and Rainey 2003) or if dominant competitors arise that suppress the output of others. However, if diversification is driven by the sequential construction of new niches — here, by the likely incidental production of metabolic byproducts that enable cross-feeding and by the production of new structures for adherence by other types — a positive association between diversity and productivity becomes more likely. These findings may help explain the role of diversity not only in structured microbial communities but also in a wide range of complex natural ecosystems in which interactions for food and living space may be common. In summary, as many biofilm researchers have speculated (Stoodley, Sauer et al. 2002; Boles, Thoendel et al. 2004; Brockhurst, Hochberg et al. 2006), biofilm productivity is positively associated with the evolution of ecological diversification.

## CHAPTER III

### ORIGINS AND MAINTENANCE OF DIVERSITY IN EVOLVING BIOFILMS: COMPETITION OR FACILITATION?

#### Abstract

It has long been thought that species diversification is driven by competition for resources and space among community members, but facilitative ecological interactions have been considered as an alternative mechanism of diversification. Because microbial biofilm populations commonly harbor diverse communities, researchers suspect that niche construction promotes diversification in environmental biofilms and in chronic cystic fibrosis lung. However, if new variants are to persist with resident populations they must occupy a vacant niche, exploit conditions produced by (facilitating) residents, or be equally as fit. In this study we examine the interactions among diverse evolved variants in experimental biofilm populations of *Burkholderia cenocepacia* to determine whether diversity arose primarily by competition or facilitation. Also, since we have previously identified the presence of synergistic behavior within our evolved biofilms we focused on dissecting the early ecological and evolutionary interactions that drove biofilm diversification by utilizing several assays of biofilm fitness. Our data indicate that diversity may evolve because mutants with slower growth rates may nonetheless be more competitive at high population density, but also because early colonists

may facilitate other mutants by nutrient cross-feeding and production of a biofilm architecture that enhances growth opportunities.

## Introduction

One of the primary goals of evolutionary ecology is to understand how different ecological processes generate patterns of evolutionary diversification. Historically, competition, either for resources or space among community members have been identified as the driving forces behind diversification, (Price 1970; Roszenschweig 1978; Rainey and Travisano 1998; Rainey, Buckling et al. 2000); however, facilitative ecological interactions, such as those between mutualistic species have been implicated (Bertness and Shumway 1993; P.E. Turner 1996; Palmer, Kazmerzak et al. 2001; Stachowitz 2001; Doebeli 2002; Day 2004; Geritz 2005). Identifying the ecological mechanisms that contribute to facilitative diversification can be extremely difficult (Hutchinson 1957; Day 2004).

Facilitation is thought to occur frequently in microbial biofilm populations due to their ability to rapidly produce diverse communities, where each unique species or variant may provide additional resources by cross-feeding or adding space as they construct biofilms (Hansen, Rainey et al. 2007) (Stewart 2008). However, direct evidence of such interactions remains lacking. Facilitation has also been implicated in driving diversification in coral

reefs and may best be seen in populations that undergo niche construction, where organisms modify their environment for their own benefit and can also promote colonization of additional species (Odling-Smee 2003). A possible explanation for the diversity seen in biofilms and other ecosystems is niche construction, where 'engineer' or resident species can alter the environment, producing new opportunities that promote other species to enter the population (Jones 1997).

The difficulty in understanding the role facilitative patterns play in species diversification lies in our inability to determine the timing, order, and causes of species diversification (Rainey, Buckling et al. 2000). Even with a known evolutionary sequence, reconstructing the selective conditions that caused evolutionary diversification is often impossible, since competition between species can either promote or prevent diversification depending on the relative benefits of specialization versus adaptation (Cooper and Lenski 2000; Rainey et al. 2000). Individuals from a single species may establish niche-specific populations adapted to pre-existing niches or new niches established by resident populations. Cross-feeding may occur if niche-specific adaptation facilitates the exchange of metabolites over space and time between metabolically unique subpopulations (Doebeli 2002). The competitive benefits of a mutualism may also allow or prevent new species invading.

One of the key mechanisms that drives competitive diversification is negative frequency-dependent selection (NFDS) (Day 2004), or the condition in which variants or species may invade populations only when they are rare. A few research groups have detected frequency dependence in experimental microbial populations started from a single genotype (Turner 1996; Doebeli 2002). Specifically, a genotype growing on one carbon source generated new metabolites that allowed additional subpopulations to utilize increasing diversity and resource utilization (Turner 1996; Doebeli 2002) or new adaptive mutations allowed growth on pre-existing resources.

Identifying the how biofilm diversification occurs under conditions promoting the reversible attachment of biofilm communities has never been examined. Therefore, in this study we examine the ecological and evolutionary dynamics of experimentally evolved biofilm populations of the CF pathogen *Burkholderia cenocepacia*. Given our previous findings that these populations evolved greater productivity, we hypothesize that selection in biofilms promotes diversification by competitive as well as facilitative interactions among newly established mutants.

### **Models for identifying competition and facilitation**

In this study, we quantified interactions, both positive and competitive, between the three distinct ecotypes (termed studded (S), ruffled (R), and

wrinkly (W)) that rose to a detectable frequency by 450 generations in each of six replicate biofilm populations. Two types of assays were used:

1. **Frequency dependence assays:** The frequency of one type (Invader) was increased while decreasing that of the other type (Resident) so that the total starting density remained constant.
2. **Density dependence assays:** The density of one type (Invader) was held constant while increasing the density of the other type (Resident), which altered both genotype frequency and density (Day 2004).

Under these conditions, if **competition** plays the primary role in generating population diversity, then the absolute fitness of both residents and invaders will decline with increasing population density (Figure 1a), but the invader will decrease in absolute fitness at a slower rate than the resident as the resident density increases.

If **facilitation** is the primary mechanism maintaining diversity, then we expect that the absolute fitness of the invader will rise with increasing density of the invader (Figure 1b). If only the resident facilitates the invader, then the fitness of the resident will decline with increasing population density, but if facilitation is reciprocal then both the relative and absolute fitness of each partner will be greatest when the other is in higher frequency and density. Such dynamics would follow NFDS, as described above, and allow each to



persist (Day 2004). In summary we emphasize that competitive and facilitative interactions are not necessarily mutually exclusive.

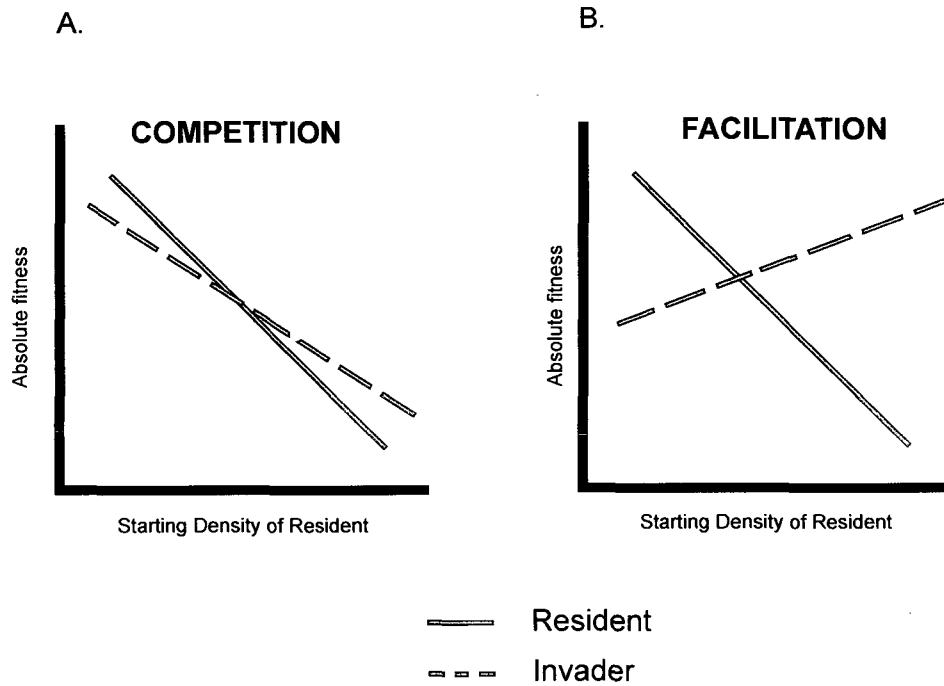


Figure 1. A. If diversification occurred because of competitive interactions, the absolute fitness of the resident type (blue line) and that of an invading mutant type (red line) will each decline with increasing density of the resident type, but the fitness of the resident will do so more rapidly, enabling successful invasion. B. Diversification by facilitation will be observed as an increase in the absolute fitness of the invader with increasing density of the resident;

meanwhile absolute fitness of the resident population declines as its density increases because of competition with itself.

Here we disentangle the relative contributions of these two processes to diversification in microbial biofilms. We find that diversity is both driven by competition for biotic and abiotic resources and facilitation by cross-feeding of metabolites and the construction of new physical niches within the biofilm environment.

### Materials and Methods

**Morphotype identification and measurement of fitness in the biofilm.** All Biofilm cells were quantified as CFU/ml from beads colonized during 24 h in 1M galactose M9 media grown at 37°C in rollerdrum (50 rpm) by vortexing beads in 1.5ml PBS for 1.5 min. Recovered biofilm populations were then plated following serial dilution on T-Soy agar plates. Colony were variants termed S, R, and W were quantified by colony counting following growth on T-Soy agar plates with colony totals over 300 for 24 h at 37°C and then 48 h at room temperature. Fitness was measured as  $\ln(N_{t=24}/N_{t=0})$  in both environments inoculated with resuspended vortexed biofilms. Colony morphology frequencies were also determined every 150 generations after they first appeared.

**Assays of frequency and density dependence.** The starting frequency of S, R, and W was altered by increasing the initial frequency of one morphotype, thereby generating three competition groups A (S9:R1:W1), B (S1:R9:W1), and C (S1:R1:W9), respectively. Cultures were preconditioned on beads in 1M galactose M9, suspended in 1.5ml of PBS and sub-cultured into new media. Assays of density dependence were completed by progressively altering the starting density of one of the morphotypes while keeping the other at a constant density (25 $\mu$ l:25 $\mu$ l, 50 $\mu$ l:25 $\mu$ l, and 200 $\mu$ l:25 $\mu$ l) and performing the opposite assay by altering the starting density of the other morphotype. Five replicate competition assays were conducted for each combination of S, R, and W and cells were recovered as described above. Fitness was measured as described above and relative fitness was calculated as the  $\ln(\text{absolute fitness of the invading rare type}/\text{absolute fitness of the abundant resident type})$  and 95% confidence intervals were calculated for each treatment condition.

**Genetic manipulations.** Fluorescent plasmids were used to identify each morphotype when grown together in biofilm populations. Plasmids pSPR (Rakhimova et al.) and pSPY (yellow) were used (Poltak and Cooper 2010), each containing a chloramphenicol (Cm) resistance cassette (Kovach et al. 1995). pSPR harbors the DsRedExpress red fluorescent protein gene and pSPY the EYFP gene (Poltak and Cooper accepted 2010). Plasmids were

electroporated into evolved morphotypes with positive selection on Tryptic-Soy Agar + 150 mg/ml Cm.

**Biofilm population dynamics.** To examine the dynamics of attachment to the bead over the growth cycle, a single mixed culture of population B1 grown overnight at 37°C in 1M galactose M9 in a rollerdrum (50 rpm) was used to inoculate 18 fresh tubes containing beads, each grown under selective conditions. Three beads were destructively sampled after 4, 8, 12, 17, 20, and 24 hours, by vortexing in 1.5 ml of PBS, dilution and plating on tryptic soy (7g/L) agar to obtain CFU/ml and morphotype frequencies at each time point and 95% confidence intervals were calculated for each treatment condition.

**Assays of cross-feeding.** Following 24 h of growth in the selective environment, cells were pelleted by centrifugation and discarded and the supernatant was purified via a 0.22mm filter. Samples (200µl) of each supernatant were added to 96 well polystyrene plates (Corning), and each genotype supernatant was inoculated with  $10^6$  CFU and incubated at 37°C for 24 hours. The optical density ( $OD_{600}$ ) was recorded every 15 min after a 5 second 2mm orbital shake. Growth in supernatant was compared to a concurrent assay of growth in the unaltered evolution medium and expressed relative to these measures. The area under the bacterial growth curve or the total area of the  $OD_{600}$  readings over time (AUC) was calculated for each

growth condition to identify the capacity of each morphotype to grow in the supernatants of other morphotypes and 95% confidence intervals were calculated for each treatment condition.

### **Confocal microscopy of interactions between morphotypes.**

Morphotypes containing either pSPR or pSPY were grown together on beads under standard selective conditions supplemented with 50mg/ml chloramphenicol to maintain plasmid. Cultures were sub-cultured from beads into selective media containing 1cm X 1cm polystyrene slides. Each culture was induced with 30ml of 10mM IPTG for 12 hours before imaging. Slides were cleaned with ethanol on one side and placed on 75 X 25 mm glass slide (Corning). DABCO (Sigma) (25mg/ml) in glycerol (0.3ml) was added to the biofilm side and a 1.5 in. glass cover slip was placed on top. Images were captured at 200X using 2048 dpi. The following excitation and emission settings were used for each marker: pSPY: 514nm/527nm, pSPR: 556/586, Z-stack images spanned from top to bottom of biofilm. Image analysis was conducted using Carl Zeiss Zen Light Edition® software.

## **Results**

### **Colony diversity arose in a predictable sequence and persisted**

Although biofilm populations exhibited colony diversity, we determined when each distinct morphotype first appeared and how their frequency changed.

The relative frequency of each new morphotype was tracked over the 1500 generations of experimental evolution in population B1 to determine the timing of biofilm diversification (Figure 2). The first variant, S, was observed at 150 generations as approximately 30% of the population. The S type rose to 50% by 300 generations as the ancestor type became rarer, and both R and W variants became detectable at approximately five each (Figure 2). S remained the dominant type over the span of 1500 generations; however, its frequency decreased between 600 and 750 generations, dropping from approximately 85% to 70%. At the same time, W increased its maximum detectable frequency to approximately 30% (Figure 2). Interestingly, S did recover from this decrease between 750 and 1050 generations, reaching its maximum frequency of approximately 98% (Figure 2).

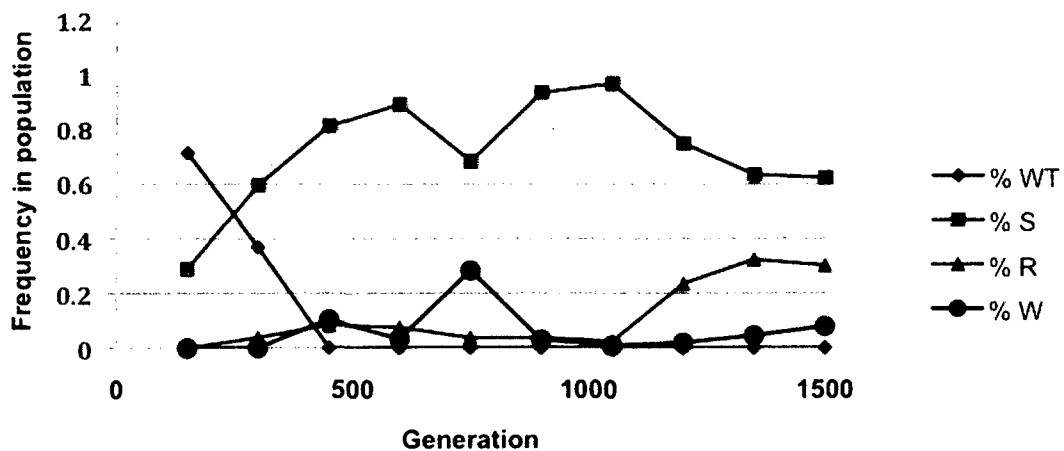


Figure 2. Dynamics of morphotype diversity within biofilm population B1 through 1500 generations of experimental evolution.

Each of the newly evolved morphotypes at 450 generations (hereafter, the Early community) was superior in colonizing the biofilm bead relative to the ancestor (Figure 3). This demonstrated that each type could drive the ancestor to extinction. We also calculated that the fitness of each type isolated at 1500 generations (hereafter, the Final community) had increased four-fold relative to the 450 generation isolates, indicating that further adaptation had occurred (Figure 3).

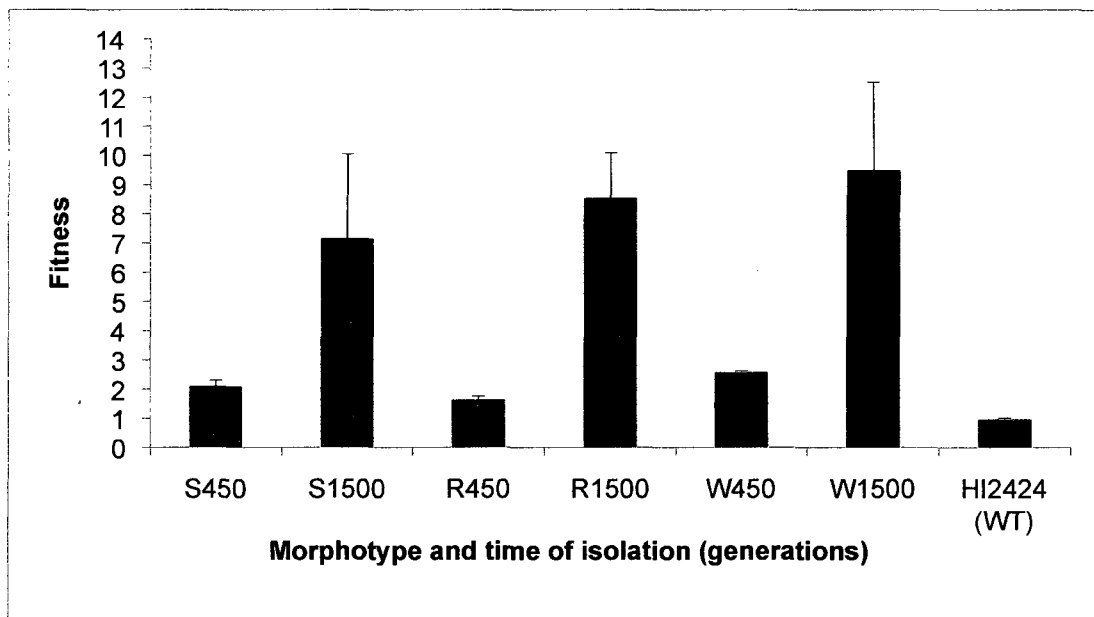


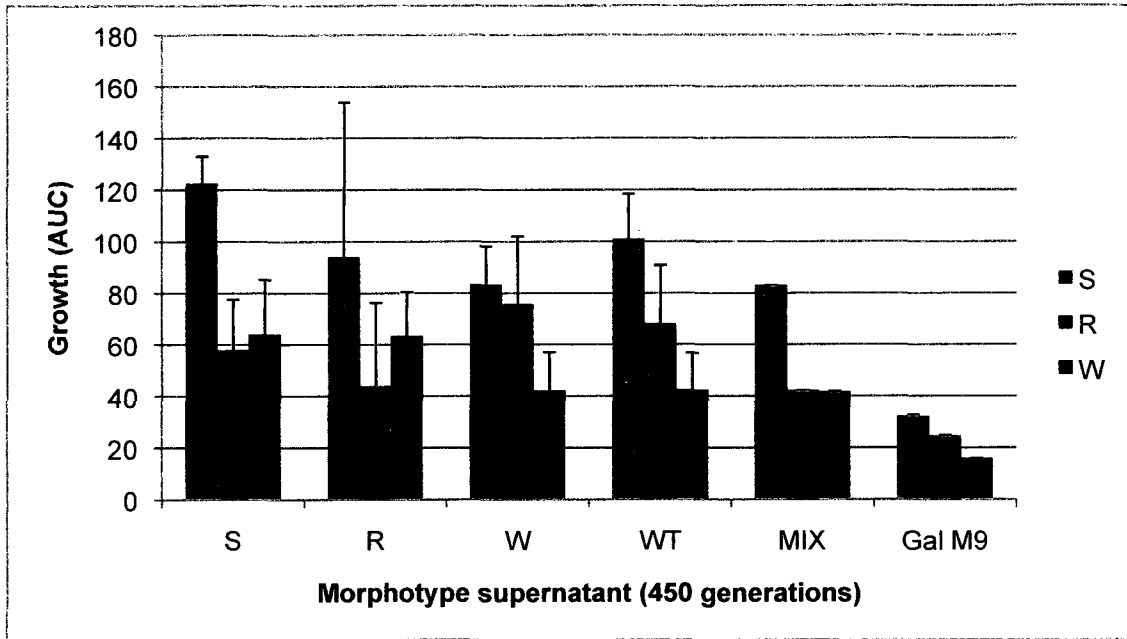
Figure 3. Relative biofilm fitness values of morphotypes from the Early (450 generation) community and from the Final (1500 generation) community versus the founding ancestor, HI2424.

### **Nutrient cross-feeding facilitates biofilm diversification**

We examined the capacity of each morphotype to grow on the metabolites of other types (cross-feeding) by growing each type in the cell-free supernatant of its community members (Figure 4a and 4b). The morphotypes collected from the Final community (Fig.4b) produced supernatants that supported more growth than those isolated from the Early community (Figs. 4a and 4b). However, both the R and W types from 450 generations were able to grow in their own supernatants (Fig. 4a) whereas the 1500-generation R and W types could not (Fig. 4b).



a.



b.

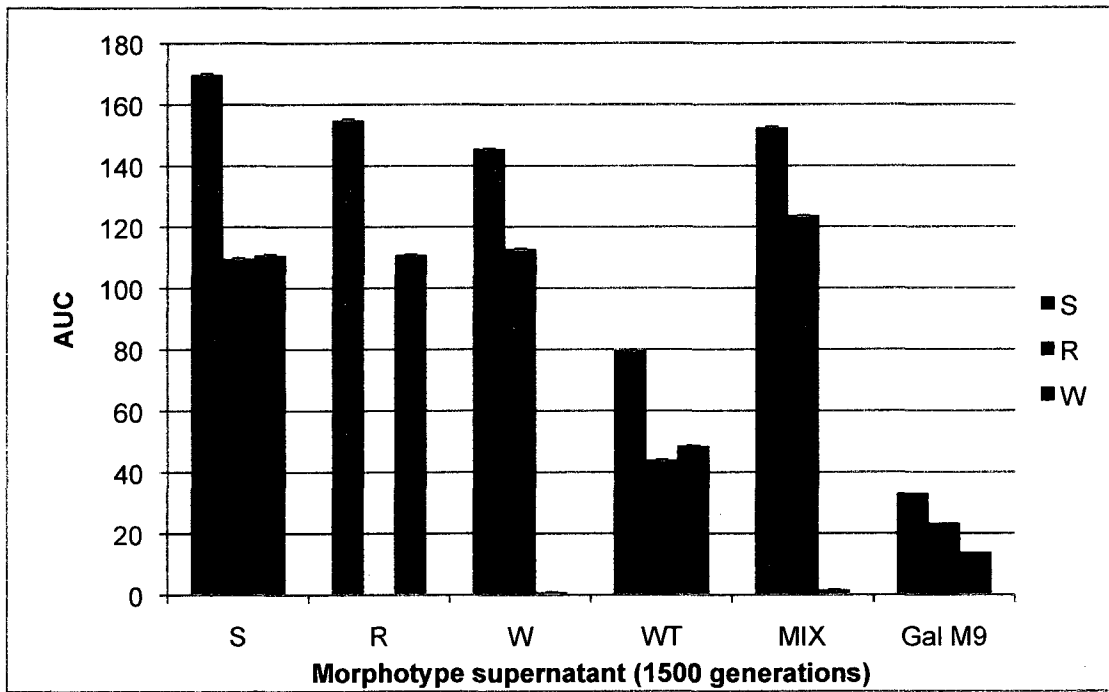


Figure 4. Benefits of cross-feeding for all pair-wise interactions between supernatant producers and consumers isolated at A. 450 and B. 1500 generations. Isolates from population B1 and the ancestor were grown in the cell-free supernatant produced by themselves and each other type. (a.) Growth was measured as the area under the curve (AUC) of OD600 over 24h,  $\pm$  95% ci, n=5. Note the increase in cross-feeding abilities of the morphotypes from 450 to 1500 generations and the inability of R and W isolated from 1500 generations to grow in their own supernatant.

#### **New biofilm colony morphotypes colonize the bead at different rates**

The dynamics of colonizing the polystyrene bead by population B1 evolved for 450 generations were observed by periodically destructively sampling the bead over the course of 24 hours. We found that each type attaches to the bead at different rates (Figure 5a): even though the S type always remains the most abundant type on the bead, the R and W types attach more rapidly to the bead between 0 and 4 hours (Figure 5a). Following this attachment the S type increases in frequency on the bead between four and 12 hours (Figure 5a) and drops between 12 and 17 hours while the R type rises (Figure 5a). All types maximized their bead colonization by 17 hours (Figure 5b).

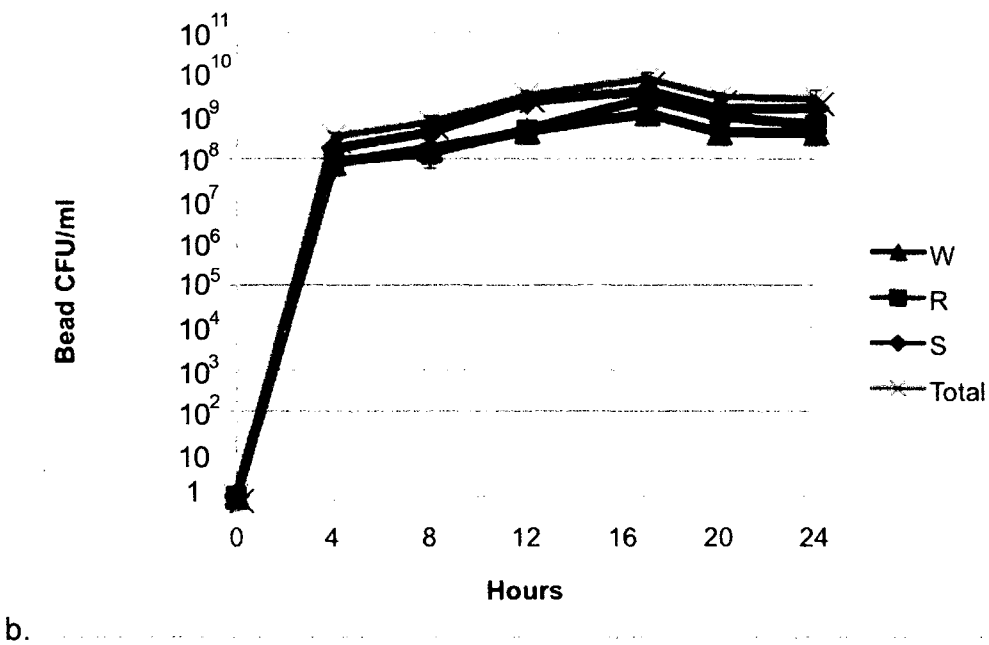
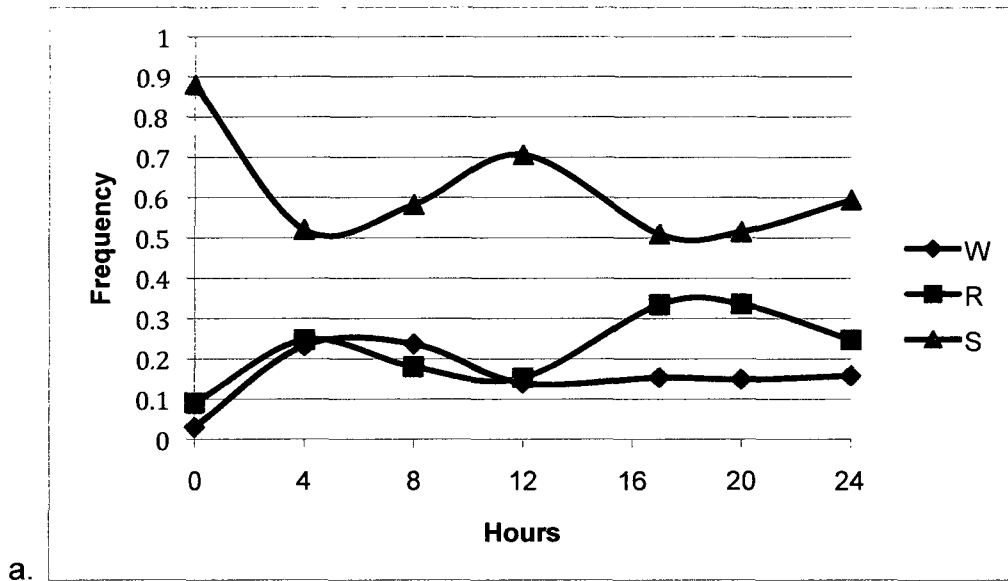


Figure 5. Dynamics of bead colonization by population B1 morphotypes from 450 generations. (a.) The frequency of each of the morphotypes (on 3 replicate beads) was measured at each time point: S (Blue), R (Green), and

W. At time zero the frequency recorded was the frequency of each type added to the culture and subsequent frequencies reflect bead colonization.

(b.) Bead colonization density. All morphotypes maximize their bead colonization density at 17 hours and slightly decline between 17 and 24 hours.

### **Fitness of evolved biofilm morphotypes depends on their starting frequency in the community**

To begin to determine the nature of the interactions in the Early evolved community, we varied the starting frequency of the dominant morphotype, S, while holding the total inoculum size constant. Thus, frequencies of R and W, both of which are superior producers of biofilm in monoculture (Poltak and Cooper, submitted), covaried as we altered S frequency. The equilibrium frequency of the morphotypes in the Early community was approximately 60% S, 30%R and 10%W. We found that altering the frequency of each morphotype affected the fitness of all three types (Figure 6). First, as the starting frequency of S increased its fitness declined, consistent with NFDS. In contrast, the fitness of both R and W increased as S became more frequent, consistent with facilitation by S, but peaked at an intermediate frequency of ~40% S (Figure 6). The W morphotype was significantly more fit than R at low frequencies of S, whereas the R morphotype was more fit than W at high frequencies of S; however, neither was more fit than S at these extreme frequencies. Because the S type

remained the most fit variant when it was common, the question of how R and W were able to invade the community remained.

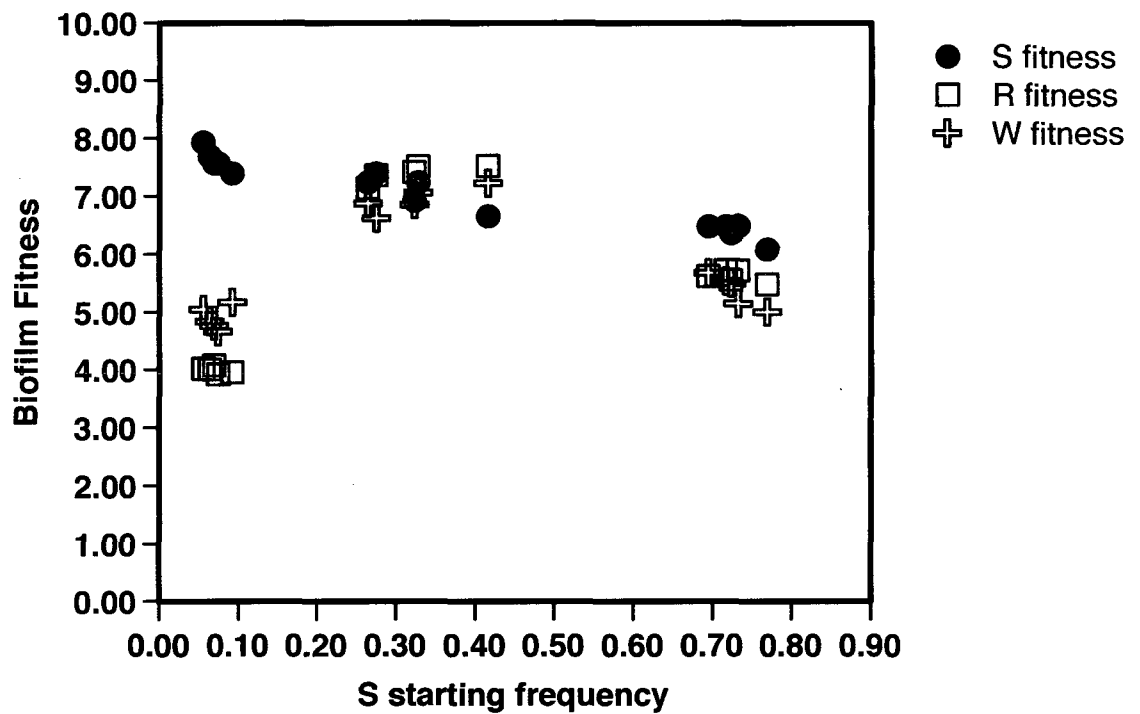


Figure 6. Fitness of the three morphotypes from the Early evolved community as a function of the starting frequency of the S morphotype. Frequencies of R and W covaried in this experiment. Fitness is the natural log of growth on or colonization of a new polystyrene bead from the starting inoculum, which was recovered from a previously colonized bead.

**Biofilm variants demonstrate both competitive and facilitative interactions in pairwise combination.**

Because the density of a resident species might influence the fitness of invading species more than their relative frequency, especially if the capacity for facilitation is density or quorum-dependent, we designed experiments that would detect such effects. For all three pairs of morphotypes from the Early community, one type ('resident') was added in increasing density (and frequency) while holding the inoculum of the other type ('invader') constant. We then reversed the roles of the mutants and repeated the experiment. Given that S was always detected first during experimental evolution and was followed by R, we began by increasing S density in combination with a fixed inoculum of R.

Under these density varying conditions, the absolute fitness of both S and R declined with increasing density of S, where S was relatively more fit at lower densities and R was relatively more fit at higher densities of S (Figure 7a, 8a). These results suggest that S and R compete but vary in their relative fitness at different densities, which would allow R to competitively invade an S monoculture. Similarly, when R density was altered and paired with constant S inoculum, R was more fit at low densities but S was more fit at high density (Figure 7a). Thus, the fitness of each is relatively greatest when its partner is

at high density (Figure 8a), even as their absolute fitness declines with increasing competition.

In pairings of R and W, as their total density increases the absolute fitness of both variants decreases, which is consistent with competition for a shared resource (Figure 7b). However, both variants demonstrate greater relative fitness at low starting densities of the other type, and R is actually inhibited at high densities of W. These dynamics are consistent with competition favoring the rarer type at low to intermediate densities of the resident population but inhibition by the dominant type at higher densities, although W appears to be less affected by high densities of R than vice versa.

In the third pairing of S and W, absolute fitness of both S and W actually increase with total density, which suggests reciprocal facilitation (Figure 7c). With increasing density of W, the fitness of S relative to W (Figure 8c) increases rapidly at low densities but then becomes equivalent at higher densities of W. Thus, S can easily invade low-density populations of W. However, with increasing S density, both the absolute and relative fitness of W increase monotonically, although with greater variance at the highest density. Such dynamics are consistent with pure facilitation of W by S, likely by the cross-feeding that occurs between these two genotypes (Chapter 2, Poltak and Cooper accepted 2010). The positive effects of W on S in turn may reflect positive interactions for biofilm assembly at intermediate densities.

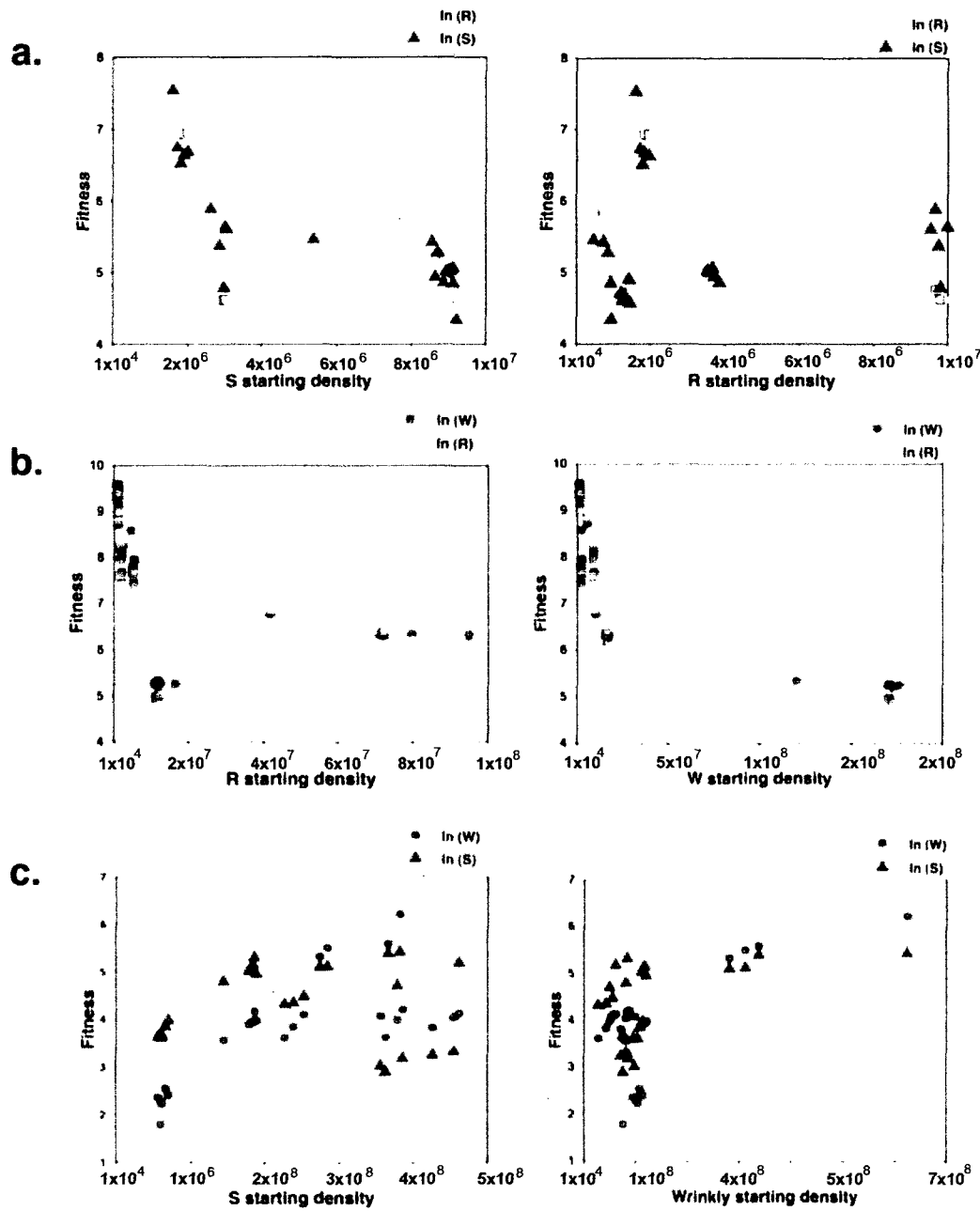


Figure 7. Absolute fitness of Early genotypes as a function of varying density of another community resident. A decline in absolute fitness by both



competitors with increasing density reflects competition (Figure 1), whereas an increase in absolute fitness at higher density of the competitor reflects facilitation. S and R and W and R combinations do not reflect pattern proposed in Figure 1; however as the starting S density is increased the absolute fitness of both competitors declines as seen in competitive interactions. Additionally, S and W do not reflect the proposed facilitative pattern in Figure 1, rather they both increase in absolute fitness when the density of either type is increased

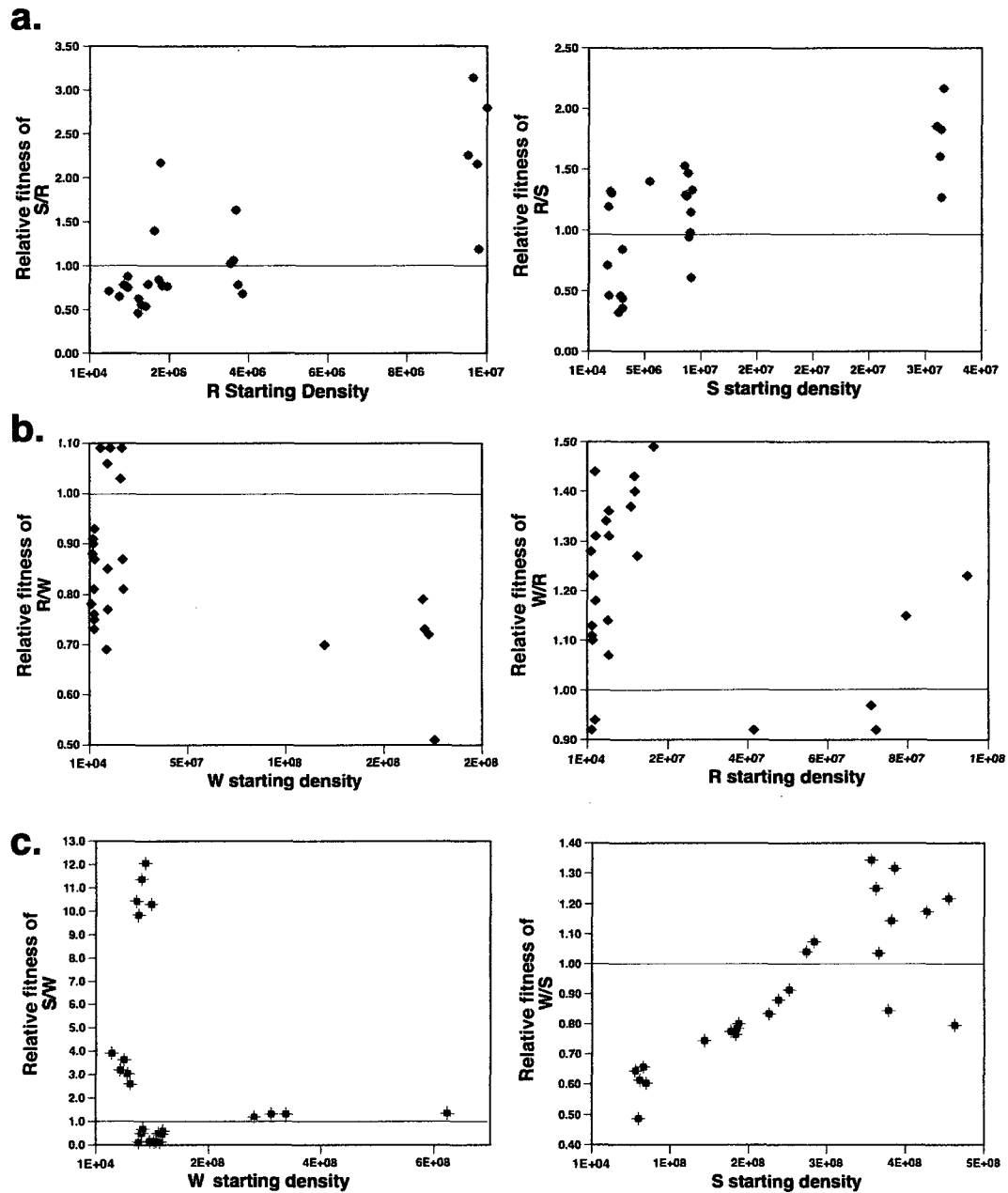


Figure 8. Relative fitness of each pairwise combination of Early genotypes as presented in Figure 7. Negative frequency-dependent selection (NFDS) is

indicated by the increase in relative fitness of an individual when its frequency is low enough (or density is high enough).

**Biofilm construction by resident types may facilitate improved attachment by other types.**

The biofilms produced by R and W in co-culture were found closely associated in microcolonies on the plastic surface (bottom view), yet the top view of the biofilm structure shows that W facilitates the attachment and growth of R at higher elevations in the confocal Z-stack. (Figure 9a).

Similarly, S is facilitated by R at higher elevations but is not essential for attachment at the polystyrene level since it coats any available surface there (Figure 9b.). Interestingly, W appears to facilitate S attachment at higher elevations, though near the polystyrene surface there is a much closer association between S and W than seen between S and R. The S and W association is clearly marked by a dense, heterogeneous foundation of S and W cells, whereas S and R cells do not mix to this extent (Figure 9c).

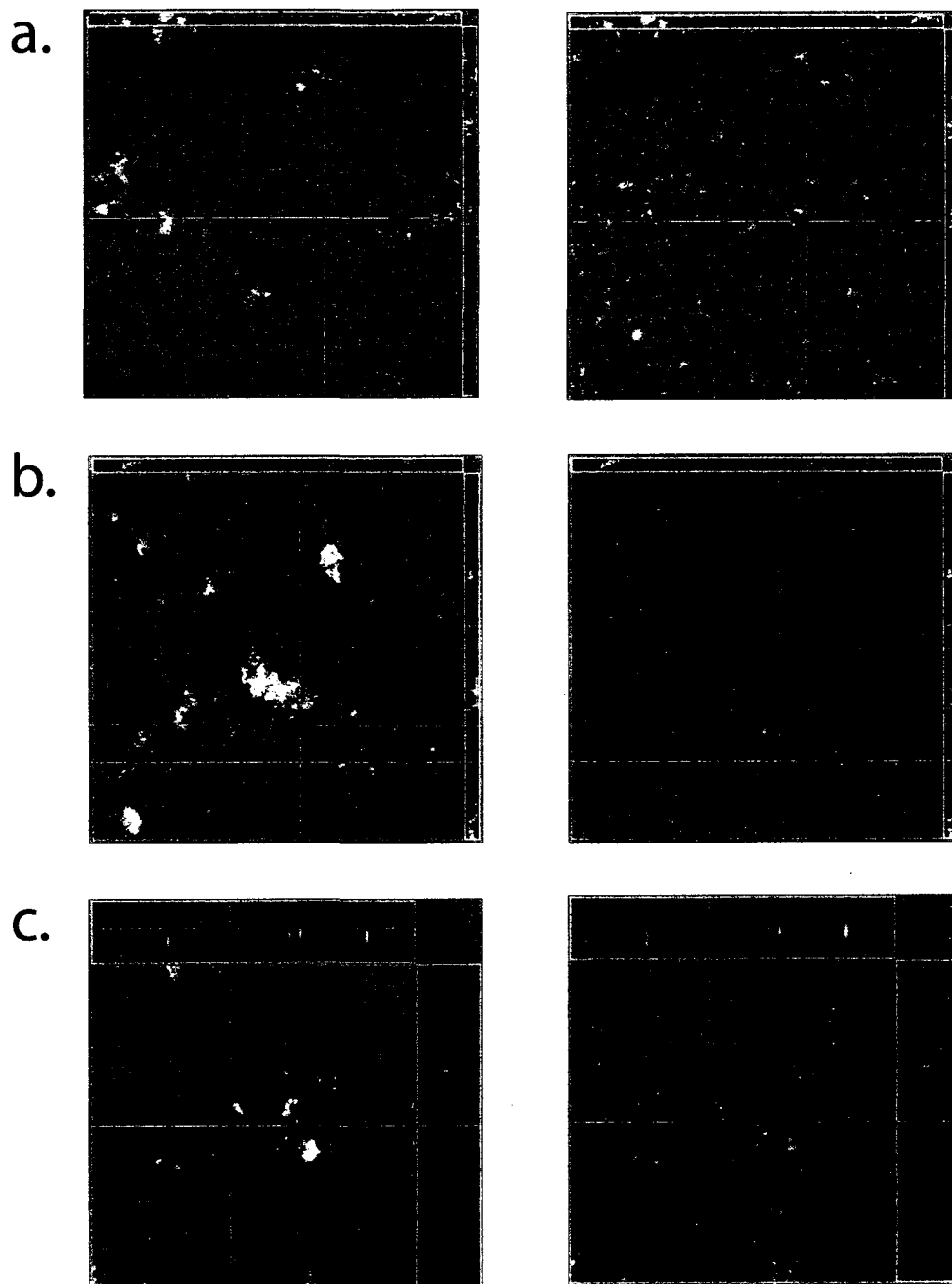


Figure 9. Confocal scanning laser microscopy of the biofilm architecture produced by mutant pairs following 450 generations of evolution. (a.) Top

layer (left) and bottom layer of R and W (green) biofilms. (b.) Top (left) and bottom of S and R (green) biofilms. (c.) Top (left) and bottom of W and S (green). The red genotype carries pSPR and the green genotype carries pSPY and is projected in green.

## Discussion

Microbial biofilm populations provide us with the unique opportunity to investigate ecological interactions such as facilitation by resident species may affect the origin and maintenance of diversity within populations (Stachowitz 2001; Day 2004). Here we directly investigated the possibility of population facilitation by cross-feeding and by structural support (Stewart and Franklin 2008).

To determine the cause of biofilm population diversification, we identified the origin of the diversity by monitoring the rise of new colony variants in experimentally evolved biofilm populations (Figure 2). As reported earlier, we found that in each of six replicate biofilm populations, colony morphotype diversity arose in a successive manner (Poltak and Cooper 2010), yet the reasons for this pattern remained unknown. In the experimental model, competition for space was unavoidable since only the cells attached to the polystyrene bead were transferred the next day. However, we also reported that long-term evolved biofilm communities exhibited synergistic behavior in biofilm population productivity, so we predicted that even early

isolates of these morphotypes might demonstrate facilitative interactions (Chapter 2) (Poltak and Cooper 2010).

Our initial evidence for facilitation beyond the increased productivity was that some types grew better in the supernatant of another type than in the unconditioned medium (Figure 4). Cross-feeding among types occurred during the daily growth period. Specifically, the S type supported significantly higher growth in its own supernatant collected after 24 hours growth than in other supernatants, and the R and W types grew better in S supernatant as well (Figure 4a-b). This phenomenon was even more apparent by 1500 generations, where R and W could no longer grow in their own supernatants, but were capable of growing in other supernatants (Figure 4b).

By monitoring the attachment timing of each type over 24 hours we also discovered that there may be a seasonal effect where certain metabolite resources become available only at certain times during the 24 hour growth period, as seen in other systems where some metabolites only are available after the growth of a primary grower (Spencer and Doebeli 2007) (Turner 1996) (Bull and Harcombe 2009). Alternatively (or concurrently), biofilm colony maturation may provide structural support to other types at specific times (Figure 5a and 9). Benefits of cross-feeding may associate with the increased relative frequencies of W and R between 0 and 4 hours (Figure 5a) and the increase in R between 12 and 17 hours. In turn, early W and R

growth on the bead may also facilitate increased S surface attachment, seen by the sudden increase in S attachment between 4 and 12 hours (Figure 5a and supported by Figure 9).

Our preliminary evidence of synergistic interactions between S, R, and W by cross-feeding and increased surface adherence led us to hypothesize that biofilm diversification is driven both by competitive and facilitative interactions. If competition or facilitation occurred between S, R, and W, then negative frequency dependence selection (NFDS) (or being able to invade when rare), would be detectable through competition assays. Therefore, we developed assays of both frequency- and density-dependence to determine if either competition or facilitation was the primary mechanism of diversification (Figure 1).

Our data show that as we increased the starting frequency and density of S, its absolute fitness declined as expected, but fitness of both R and W types increased as the facilitative effect of S rose in the population (Figure 7). However, when the initial frequency of S exceeded 40%, these potential facilitative effects of S were diminished, most likely due to antagonistic effects of S competition. Further potential NFD effects of both R and W on S were observed with increasing initial density of R and W, thereby allowing S to colonize the bead much more efficiently (Figure 9a and 9c). However, even though R and W improved the absolute fitness of S as their starting frequency increased, fitness of all types eventually declined (Figure 7). We speculate

that this decline is either to increased competition for space or to a disruption in cross-feeding on secondary metabolites.

Our results also define a likely mutualism between the S and W types because increasing the density of either type while maintaining a constant density of the other increases absolute fitness of both types (Figures 1 and 7c). This observation of the evolution of a *de novo* mutualism between co-evolved genotypes is nearly unprecedented (Turner 1996), especially in the absence of external selection. This dynamic also demonstrates the potential for synergistic coevolution in biofilms in addition to the social cheating that has been well described (Rainey, Buckling et al. 2000; Brockhurst, Hochberg et al. 2006; Brockhurst, Buckling et al. 2007; Harrison and Buckling 2009; Ross-Gillespie, Gardner et al. 2009). The mutualism likely results from cross-feeding that favors W (Figure 3) and biofilm structural support that favors S (Figure 9).

In contrast to the cooperative interactions between S and W (Figure 7c), the relationship between R and W proved to be exclusively competitive (Figure 7b). R was found to facilitate S, but S does not do so in return (Figure 7a) and R facilitates S in structural support and attachment at higher biofilm elevations and S shows no biofilm structural support for R (Figure 9b). The absolute fitness of both R and W declined with an increase in starting density of either type, and showed low potential for NFDS (Figure 8). This result may



have occurred because R and W colonized the surface of the bead similarly (Figure 9a-c), resulting in competition for available space, or because the removal of S eliminated its facilitative effects on R and W.

Competition for space and resources between species as a driving force for adaptation has been relatively simple to quantify in comparison to facilitation. Diversification due to facilitation may be difficult to detect because such interactions may be sensitive to shifts in population densities and environmental conditions. Here we show that facilitation is indeed sensitive to starting conditions because only certain starting densities of each morphotype produced facilitative interactions between S, R, and W.

More broadly, we have presented the first study to provide evidence that both competitive and facilitative interactions may favor diversification of a single ancestral genotype into distinct colony morphotypes (and ecotypes) during biofilm selection. Our evidence further suggests that diversification of biofilm species is driven by competition for biotic and abiotic resources as well as facilitation by cross-feeding and biotic niche construction. In conclusion, we suggest that the ecological and evolutionary dynamics of facilitation observed in this system will help us to better understand community biodiversity and stability in other diverse ecosystems (Bertness and Shumway 1993; Palmer, Kazmerzak et al. 2001; Stachowicz 2001).

## CHAPTER IV

### EVOLUTIONARY GENETICS OF BIOFILM ADAPTATION BY *BURKHOLDERIA CENOCEPACIA*

#### Abstract

The extent of genetic variation in a biofilm population could be the result of several evolutionary forces; however, accessible sequencing technologies now offer new opportunities to discover and characterize the diversity found in evolving microbial populations on the whole-genome scale. By sequencing biofilm mixed-population samples and morphotype clones, we have identified several mutations present at various points in the history of a *B. cenocepacia* population that has evolved for ~1500 generations from a founding clone. With up to 200-fold genome coverage, we were able to identify potentially beneficial mutations as they swept to fixation, discover contending beneficial alleles that were potentially eliminated by clonal interference, and detect other minor variants possibly adapted to new ecological niches.

#### Introduction

Adaptation is the basis of much of the biological diversity that we see in nature, but identifying the molecular bases of adaptation can be extremely difficult. The study of model organisms in controlled environments allows us to reduce the variables often encountered in nature and may better highlight

the mutations that underlie adaptation to those conditions (Elena and Lenski 2003). In addition, the advent of new sequencing technologies has enabled the identification of all genetic changes that occur during the course of microbial evolution experiments (Velicer, Raddatz et al. 2006; Barrick, Yu et al. 2009; Beaumont, Gallie et al. 2009). To date, only a few groups have exhaustively identified the beneficial mutations that occur during the experimental evolution of bacteria (Velicer, Raddatz et al. 2006; Barrick, Yu et al. 2009; Beaumont, Gallie et al. 2009), and no study has identified the mechanisms of adaptation during long-term selection in biofilms, perhaps the predominant lifestyle of microbes.

Microbial biofilms are known to generate and maintain higher biodiversity and exhibit greater spatial and physiological heterogeneity than planktonic populations (O'Toole, Pratt et al. 1999; Hall-Stoodley, Costerton et al. 2004; Stewart and Franklin 2008). Of greater concern is that many human related bacterial infections are attributed to biofilms (Hall-Stoodley, Costerton et al. 2004; Palmer, Mashburn et al. 2005). Therefore, in this study we have focused on the adaptation of *Burkholderia cenocepacia*, an opportunistic pathogen responsible for fatal chronic biofilm-associated lung infections in cystic fibrosis (CF) patients (Coenye, Spilker et al. 2004; Mahenthiralingam, Urban et al. 2005), to a biofilm environment. Although this species has been identified as the most prevalent in CF patients and is the most pathogenic among all the *Burkholderia cepacia* complex (Bcc) species (Coenye, Spilker

et al. 2004), little is known about how it adapts to a biofilm lifestyle or to the CF lung environment.

Each of six *B. cenocepacia* populations underwent 1500 generations of biofilm selection diversified into very similar sets of three distinct colony morphotypes from a single ancestral genotype. Interestingly, previous studies have shown that at least one of these colony morphotypes – a small, highly rugose “wrinkly” type – is commonly isolated from chronic lung infections of both *Burkholderia* spp. and *Pseudomonas aeruginosa* and are known to be associated with high patient mortality (Haussler, Lehmann et al. 2003).

We hypothesized that under biofilm selective conditions, mutations in pathways known to be important for biofilm production such as those involving regulation of quorum sensing (QS) (Huber, Riedel et al. 2002) and exopolysaccharide production (Sist, Cescutti et al. 2003) would be favored. We obtained and compared the complete genome sequences of clones of each of three distinct colony morphotypes, studded (S) type, ruffled (R), and wrinkly (W), to the ancestral genotype, *B. cenocepacia* strain HI2424 (Coenye, Spilker et al. 2004; Poltak submitted 2010). In collaboration with the Joint Genome Institute (JGI), we also obtained metagenome sequences from samples of the mixed population in which these clones evolved at three

evolutionary time points: 450 generations, 1050 generations, and 1500 generations.

These genome and population sequences invaluablely identified many mutations associated with adaptation, but to associate these alleles with certain morphotypes, to define haplotypes, and to track their frequencies, we also screened 10 clones of each morphotype at generations 750 and 1500 for several evolved alleles. From these analyses we were able to reconstruct the evolutionary history of adaptation and diversification in a single biofilm population, in which multiple lineages acquired mutations in the same genes that were likely adaptive. Several of these mutations occurred in genes that had previously been found in isolates of *P. aeruginosa* from chronic lung infections, which implies that experimental biofilm selection on populations of *B. cenocepacia* may mimic biofilm selection in general and contribute to our understanding of adaptation during chronic infections. We also identified multiple adaptive lineages that each produced distinct biofilm ecotypes and coexisted for hundreds of generations, which may explain the exceptional biodiversity of natural biofilms including those associated with chronic infection.

## Methods

**Culture conditions.** Throughout the long-term *B. cenocepacia* biofilm

evolution experiment, a 1 ml sample of each mixed population was stored at 80°C in 15% glycerol. Mixed populations and individual clones were re-propagated by growing them for 24 hours in 15x180mm test tubes containing 5ml of M9 medium + 1M galactose combined with 1ml tryptic soy broth added. All cultures were spun using a rollerdrum at 50 rpm.

**Genomic DNA isolation.** DNA was collected and purified by an ammonium acetate salting out method (Miller 1988) using 5ml of culture and resuspended in TE buffer for further analysis.

**Mutation detection.** Single S, R, and W mutants were selected from a plating of population B1 from 1500 generations of the experimental evolution and following growth in 1M galactose M9 medium. Purified genomic DNA was resequenced by Illumina Genome Analyzer sequencing performed by the Joint Genome Institute, US Dept. of Energy, Walnut Creek, CA. The 7.8Mb genome of each mutant was sequenced to with over 100x coverage. Mutations were identified in the first pass from the most conservative run of eland (Illumina) and then more were identified using MAQ (Li, Ruan et al. 2008), using the output of a minimum mapping quality of 20.

**Quantifying short nucleotide polymorphism (SNP) mutations.** To confirm SNPs, primers flanking putative mutations were designed to amplify the region using PCR. The genes *yciR*, *manC*, *bfr*, *wspA*, and *wspD* in ten

isolates of each morphotype from time points 750 and 1500 were screened for the mutations previously found by Illumina sequencing. Mutated regions were aligned in MEGA 4 (Kumar, Nei et al. 2008). The PCR primers, used (5'-3') were as follows: bacterioferritin (*bfr*): Forward AGACGATGCTCGCTCAGA, Reverse CTTCAGGTCGCACTTCAGG. *yciR*: Forward TGACGGCAATCACGGCAG, Reverse ATCTACACGGGCTTCGGCAC. *manC*: Forward GCGGTGTGGCGGAGTATG, Reverse: GTCGCTTGCGTCGTCTGAA. *manC* sequencing primer CGTGTCGGAAGGTGGTTACTG. *wspA*: Forward CGCACGATGAACGAAGT, Reverse GCACCTCGGCGATGAT. *wspD*: Forward CGCCGCCACTGACGA, Reverse TTGCCACGCCACGACA.

Single nucleotide variations (SNVs) and putative small insertions or deletions were identified using maq-0.7.1 (Li, Ruan et al. 2008; Ruan, Li et al. 2008) mapping short DNA sequencing reads and calling variants using mapping quality scores. Notes on nomenclature: We have chosen to use the term Single Nucleotide Variant (SNV) instead of Single Nucleotide Polymorphism (SNP) because many variants do not fit the strict definition of polymorphism.

### **Calculating selection rate constant of mutations**

In order to quantify the selective rate of each mutation, we estimated  $r$  from the equation  $dP/dt / (P*(1-P))$  where  $P$  is the frequency of the selected allele

and the maximal selective rate constant (Figure 2).

### **Colorimetric iron assay quantifies intracellular iron concentrations**

Several genes involving iron metabolism and storage were identified by genomic sequencing, therefore the intracellular iron concentrations were quantified to identify variations among genotypes. Cultures were grown to exponential phase in M9 minimal medium + 1M galactose; cells were then pelleted and washed twice in ultrapure water. Nitric acid (3%) was added to cells in a 1.5ml polypropylene tube and incubated for 16h at 98°C and then centrifuged 12,000rpm for 5 min (Tamarit, Irazusta et al. 2006). Supernatant (400µl) was added to 320µl of BPS, 160µl of 38mg/ml sodium ascorbate, and 126µl of ammonium acetate (saturated diluted to 1/3) and incubated for one minute. The non-specific absorbance (680nm) and the iron chelator absorbance (535nm) were measured. Intracellular iron was calculated as absorbance at 535nm value- absorbance at 680nm (Tamarit, Irazusta et al. 2006).

## Results

### **Identification of mutations associated with biofilm adaptation and diversification**



Each of six populations was founded by a single clone of *B. cenocepacia* and thus all evolved variation during biofilm selection arose *de novo*. Our strain (HI2424) in principle is capable of recombination since both ancestral and evolved genomes contain a plasmid. However, our analyses of the sequenced genomes and alleles do not reveal any evidence of recombination but rather support a model of sequential mutation on a common genomic background (Figure 1).

Complete genome resequencing of each morphotype clone and the sampled B1 mixed population yielded 37 confirmed or high-probability mutations at 1500 generations: 23 non-synonymous substitutions, six found in promoter regions, four deletions, and four silent single nucleotide polymorphisms (SNPs) (Table 5). The preponderance of mutations causing likely functional change in coding sequences provides strong evidence that most were favored by selection. Despite the high number of mutations detected in the mixed population, a genomic background comprised of mutations m1- m6 (Table 1) dominated the population by 1500 generations at a frequency of 97% and was detected within each of the three morphotypes, which defines their shared ancestry. Nine mutations were found to be morphotype-specific whereas the remaining 22 mutations have not yet been

attributed to specific morphotypes (Table 2).

Mutation #	Annotation	Chromosome	Chromosome Position	Gene Position	Ref. > Consensus	Mutational effect	JGI GID	Studded (S)	Ruffled Spreader (R)	Wrinkly (W)
m1	2-oxoglutarate dehydrogenase ( <i>ogdh</i> )	1	1669345	610	C > A	R > S	639693549	X	X	X
m2	95 gene deletion*	2	397098..494098	na	deletion	na	na	X	X	X
m3	<i>lysR</i> transcriptional regulator	1	927533..927539	6bp deletion 5' to <i>ldh</i>	deletion	frameshift of 2 codons	639692850	X	X	X
m4	<i>manC</i>	1	983597	771	deletion	missense, premature stop, polar effects	639695848	X	X	X
m5	<i>mscS</i>	1	2342497	405	C > T	silent	639697323	X	X	X
m6	bacterioferritin (-10 promoter region) ( <i>bfr 37</i> )	1	2447744	37 bp 5'	G > A	na	639694253	X	X	X
m7	49 gene deletion**	2	1517098..1576098	na	deletion	na	na	X		
m8	succinate dehydrogenase ( <i>sqr</i> )	2	815573	441	T > C	silent	639695995	X		
m9	<i>wspD</i>	2	650224	103	C > T	L > P	639695848		X	
m10	aminoglycoside transferase operon ( <i>rhlB</i> homolog)	1	1966500	90 bp 5' of operon	G > C	na	639693813		X	
m11	<i>mltA</i>	1	597795	18 bp 5'	G > A	na	639692556		X	
m12	DUF88	1	1310899..1312395	624	G > C	A > P	639693229		X	
m13	<i>wspA</i>	2	647269	587	C > T	A > V	639695844			X

**Table 1.** Mutations detected by Illumina genome resequencing of a single representative clone of each morphotype following 1500 generations of biofilm experimental evolution. \*m5 gene content is described in Table 6 and \*\*m6 gene content is described in Table 7.

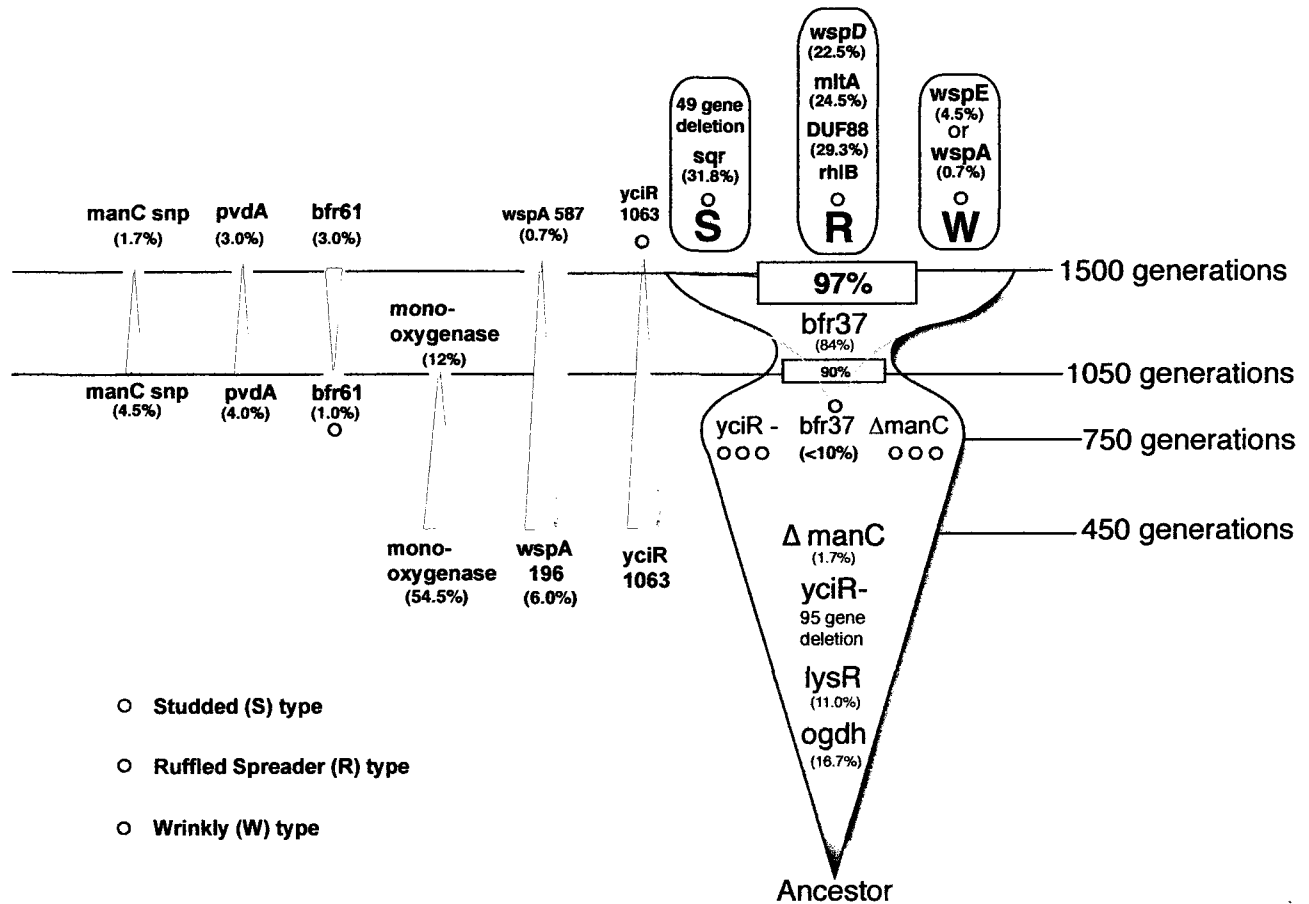


**Figure 1.** Mutational dynamics within a population of *Burkholderia cenocepacia* during 1500 generations of biofilm selection (allele frequencies in parentheses). Mutations within the shaded region define the dominant genomic background that ultimately constituted 97% of the population. Coexisting mutations (red arrows) are associated with less abundant lineages that persist in multiple samples. Boxes (above) around S, R, and W define mutations unique to resequenced isolates of these mutants. Note that the *bfr37* mutation first found in a S clone at 750 generations is associated with a selective sweep that remodels all ecotypes. Allele frequencies not shown could not be estimated from the metagenome information because they involve deletions.

**An ecologically and functionally diverse biofilm population shares a common set of mutations**

Each of the three sequenced morphotype clones, S, R, and W, shared six mutations: a SNV in a gene encoding 2-oxoglutarate dehydrogenase (*ogdh*) (m1), a 95-gene deletion (m2), a deletion of two codons in a gene annotated as a putative *lysR* transcriptional regulator (m3), a single base deletion leading to an early stop codon in the *manC* gene (m4), a synonymous mutation in the *mscS* gene (m5), and a SNP in the -10 promoter region of a gene encoding bacterioferritin (*bfr37*) (m6) (Table 1). By 450 generations mutations m1-m4 were detected in the metagenome at frequencies of 1% to 16% and by 750 generations isolates of all morphotypes were found to share this genomic background, though not exclusively (Figure 1). At this time, the m6 mutation was first detected in this lineage but only in a single S isolate (Figure 1). By 1050 generations, 90% of the population contained mutations m1-m5 and 84% also had acquired m6, which demonstrates a rapid sweep indicative of positive selection (Figure 1). By 1500 generations 97% of the population shared the m1-m6 genetic background; the remaining 3% possessed alternative genomic backgrounds were found only in S and W morphotypes (Figure 1).

### **Biofilm population genetics: calculating the force of selection on several alleles in the dominant genomic lineage**

We calculated the selection rate constant,  $r$ , for mutations m1, m3, m5, and m6 to track the selective advantage of each mutant allele in the dominant

genomic lineage (Lenski 1991; Nagylaki 1992) (Figure 2). This value will rapidly increase, plateau, then decline for any allele (typically a beneficial mutation) sweeping to fixation in a population. Based on the frequencies of these alleles in the metagenome, the m1 mutation likely arose first followed by mutations m2, m3, m4, and m5, and m6 (Figure 1 and Table 6). Our estimation of  $r$  supports this model of sequential fixation, as the maximal selective rate constant of m3, m5, and m6 occurs after the maximum rate for m1 (Figure 2). The strong correlation in the rate dynamics for m1 and m5 also suggests that m5, which is silent, rose to fixation by hitchhiking on the m1 clonal background. Finally, the selection rate constant value of m6 remains high by 1500 generations since it had not yet completely swept the population.

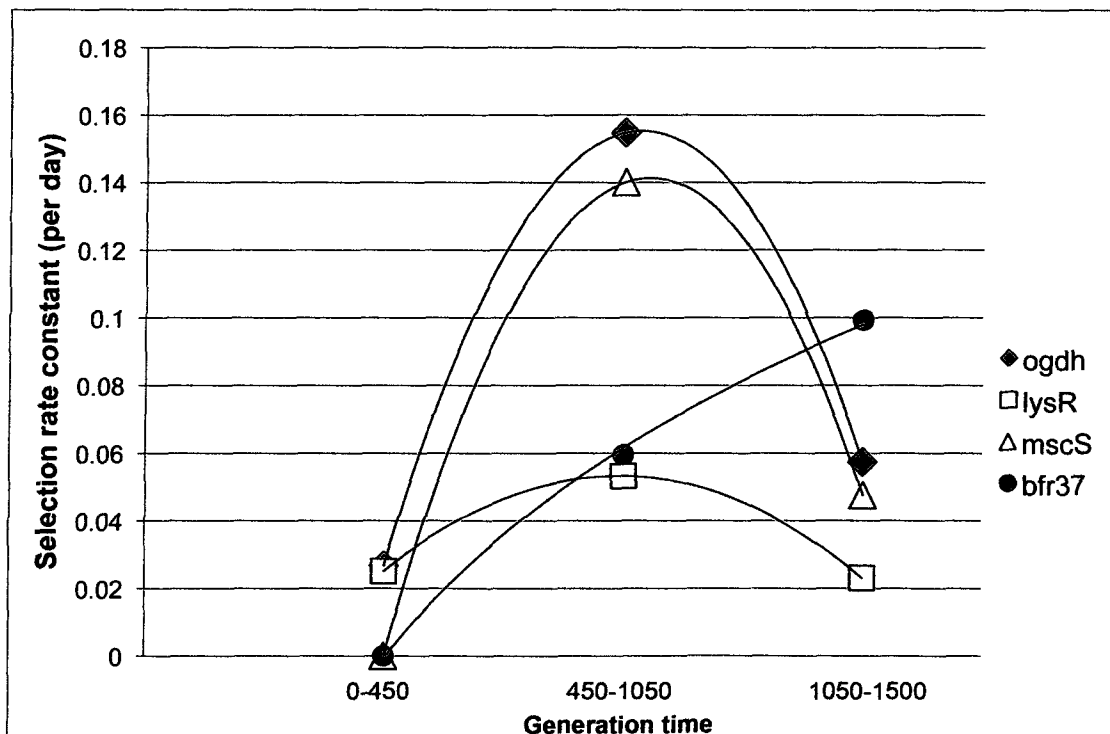


**Figure 2.** Selection rate constant of each gene associated with the dominant genomic lineage in population B1 calculated for three specific time periods (Lenski 1991; Nagylaki 1992). Alleles *ogdh*, *lysR*, and *mscS* increase in their selection rate constants then decrease as they become dominant in the population and likely encounter clonal interference from competing beneficial lineages. Note that the *bfr37* allele selection rate constant increases rapidly through 1500 generations likely by a single selective sweep from an S clone with this dominant genomic background (Figure 1).

### **Multiple mutations occurred in the same genes and define common targets of selection**

Although a common genotypic background evolved to dominate the population, alternative genotypes associated with S, R, and W morphotypes also evolved and persisted for much or all of the experiment. For example, a second mutation in the bacterioferritin promoter region (*bfr61*), mapping approximately to the -35 position of the promoter, was detected in 90% of W isolates screened at 750 generations and at ~3% of the metagenome at 1500 generations. By comparison, 97% of the population, and all W isolates screened at 1500 generations, shared the *bfr37* allele. Similarly, a second nonsynonymous substitution in *manC* distinct from m4 and in the phosphomannose isomerase domain of this protein was detected at 1050 generations (Table 1). Two distinct mutations in the gene homologous to *wspA* in *Pseudomonas* (D'Argenio, Calfee et al. 2002; Boles, Thoendel et al. 2004) also occurred: nonsynonymous substitution N196I was found at 6% in the metagenome from 450 generations but at <1% at 1500 generations, and

substitution m8 (A406V) was found in the sequenced W isolate at 1500 generations.

Interestingly, the 95-gene region that was deleted in a large fraction of the population contains two genes (*yciR* and FAD-binding monooxygenase) that acquired favored mutations in clones in which the large deletion did not occur. First, we found two nonsynonymous substitutions in a gene annotated as *yciR* that encodes a GGDEF/EAL protein and is predicted to regulate concentrations of the bacterial second messenger, cyclic-di-GMP (Huber, Riedel et al. 2002). One substitution was found at position 316 in a probable scaffold domain at a frequency of ~15% in the 450 generation sample, but this allele was not detected at later time points and was likely eliminated by superior adaptive lineages. A second substitution was found at position 1063 in the GGDEF (diguanylate cyclase) domain at a frequency of 63% in the 450-generation sample and remained detectable for the remainder of the experiment, although its proportion clearly declined as the large deletion of this region (m2) rose to high frequency. These two substitutions in *yciR* viewed in combination with the m6 deletion, in which *yciR* is the first gene deleted, underlines its exceptional significance to adaptation in this system. Second, a nonsynonymous substitution in a gene predicted to encode a FAD-binding monooxygenase was found at a frequency of ~53% in the 450-generation sample and also remained detectable for the remainder of the experiment, but again became quite rare owing to the dominance of the m2

deletion. In sum, a total of six different alleles were found in genes that were mutated in the dominant (m1-m6) adaptive lineage, which provides strong evidence that alterations in these proteins were favored by biofilm selection.

### **Alternative lineages evolved in the biofilm populations but remained rare or became extinct**

After 450 generations of biofilm selection, 14 high-confidence mutations (Table 2) were found in the population but only three ultimately defined the dominant adaptive lineage, which implies that an early period of rapid diversification occurred and was followed by selective sweeps that reduced much of this variation. Nevertheless, two of these 11 'minority' mutations survived these sweeps: a nonsynonymous substitution (T481A) in a gene annotated as a monooxygenase remained detectable through 1050 generations and the *wspA* 587 allele persisted through 1500 generations (Figure 1 and Table 2).

By 1050 generations, eight out of eleven new mutations were found outside the dominant lineage with only four detectable by 1500 generations: *bfr61*, *yciR* 1063, *pvdA*, and the *manC* SNV (Figure 1). Interestingly, both the *bfr61* and *yciR* 1063 mutations were found only in specific morphotypes. The *bfr61* mutation is exclusive to the W type from 750 to 1500 generations and



the *yciR* 1063 mutation was detected only in S morphotypes at 1500 generations (Figure 1). The periodic rise and fall of mutations outside the dominant lineage demonstrates the effect of the sweeps occurring within that lineage on the overall population diversity. Although distinct lineages clearly persisted throughout the experiment, they along with numerous low-frequency alleles were driven to the minority. This purging of diversity occurred despite the high probability that most of these alleles were beneficial because they were nonsynonymous and would not otherwise be detectable in such a large population (effective population size,  $N_e = 5 \times 10^8$ ). It is perhaps more notable that the selective sweeps were incomplete, suggesting that the structured biofilm environment may have enabled multiple adaptive lineages to persist over hundreds of generations in the face of strong selection.

### **Altered iron metabolism and storage was favored by selection**

Iron has been shown to be a key limiting nutrient in biofilms (Hall-Stoodley, Costerton et al. 2004), so it was not unexpected that several mutations shared among morphotypes were found to involve iron metabolism. The m3 mutation involves a SNV 37 base pairs 5' to the translational start and 10 bp 5' to the transcriptional start of the bacterioferritin gene (*bfr*) (gene ID 639694253), which encodes an iron storage protein that forms 24-subunit complexes that store iron as a homomultimer (Tsugita and Yariv 1985;

Andrews, Harrison et al. 1989; Davis, Elisee et al. 1999). Three additional genes involved in iron metabolism were lost in all morphotypes as part of the m6 deletion. These genes consisted of one of several ferredoxin genes (gene ID 639695680) present in the ancestral genome, a Rieske iron-sulfur binding protein (gene ID 639695678), and a ferredoxin iron-sulfur binding domain protein (gene ID 639695690), all of which are involved in electron transport (Bruschi and Guerlesquin 1988)(Table 6)

Several other mutations related to iron metabolism were detected in our metagenome analysis but not in the fully sequenced clones, including the alternative promoter mutation in bacterioferritin (*bfr61*), the second ferredoxin gene (gene ID 639698830), a ferric iron ABC transporter gene (gene ID 639693246), the *pvdA* gene involved in siderophore production (gene ID 639693688) and a probable Fe-S binding protein (gene ID 639696306) (Table 2). As stated previously the *bfr 61* SNV was found only in the W type, however the haplotypes of the other morphotypes present at that time remain uncertain. These rare alleles related to iron metabolism suggest that alternative modes of metabolizing iron may be beneficial especially if they improve competition or storage at low frequencies.

Given this evidence that selection favored altered iron metabolism, we quantified the intracellular iron concentrations of ten isolates of each morphotype from 1500 generations and found that each type contained significantly less intracellular iron than the ancestral genotype. These results

suggest that the loss of genes related to iron metabolism may contribute to this reduction. We emphasize that the ancestral genotype harbors more iron than the blank media controls, which suggests that it can sequester the available iron; thus, adaptation in this system may have favored reduction in iron uptake from a high starting condition; however, our assay only detects soluble intracellular iron.

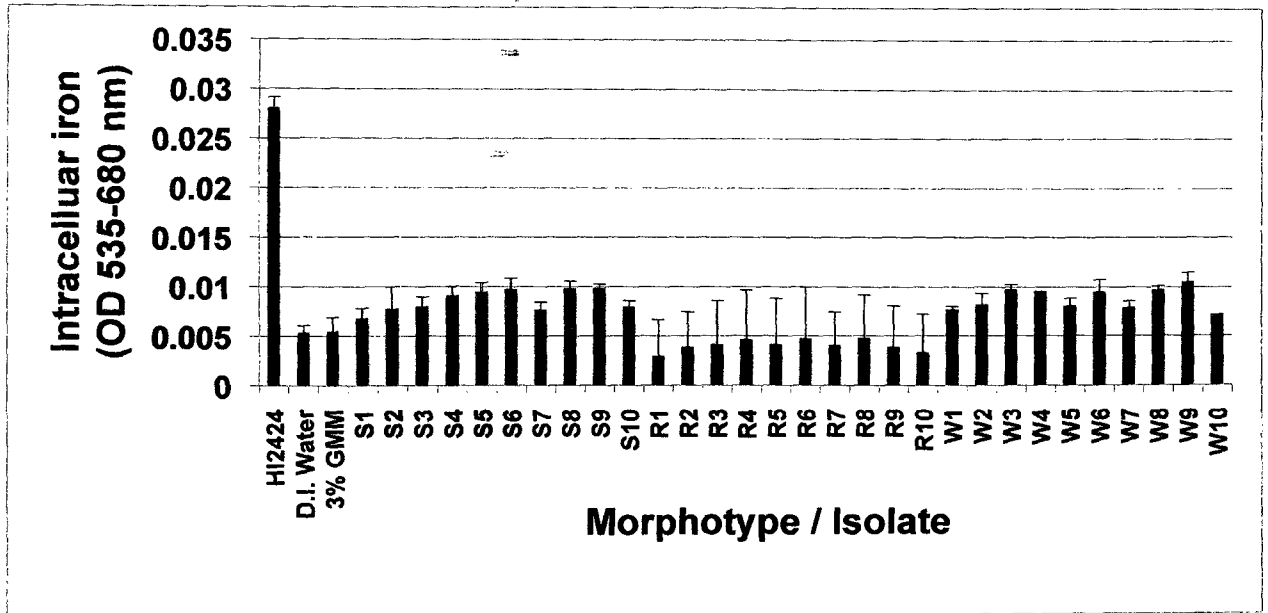


Figure 3. Intracellular iron concentrations of ten isolates of each morphotype isolated from population B1 at 1500 generations. All isolates exhibit significantly less intracellular iron relative to the ancestral genotype with no significant differences quantified between morphotypes. Error bars indicate 95% c.i.

**All morphotypes share a deletion in *manC*, a gene necessary for the production of the biofilm polysaccharide cepacian**

A mutation in the mannose-1-phosphate guanylyltransferase gene (m4) involved a single base deletion at gene position 771, which caused a missense mutation. The function of the wild-type enzyme is bifunctional and encodes both a phosphomannose isomerase (PMI) domain and a GDP-D-mannose pyrophosphorylase (GMP) domain (Jensen and Reeves 2001). The mutation disrupted the PMI domain, which catalyzes the reversible isomerization of fructose-6-phosphate (F-6-P) and mannose-6-phosphate (M-6-P) (Jensen and Reeves 2001). The second enzymatic function of *manC* is the which incorporates a GTP molecule into M-1-P, yielding GDP-D-mannose and free pyrophosphate (Jensen and Reeves 2001). Theoretically, this domain may still be functional in our evolved mutants and now overproduce GDP-D-mannose that is then used in the biosynthesis of cepacian, a repeating polymer of glucose, galactose, fucose and glucuronic acid, which is important in biofilm construction (Gottesman and Stout 1991) (Sist, Cescutti et al. 2003) (Davies and Geesey 1995).

### **Mutations unique to biofilm morphotypes likely define the phenotypic form and function**

In addition to the six mutations shared by all morphotypes, ten of the 37 mutations identified by sequencing clones of each morphotype were unique to that morphotype. Of these ten mutations, three were specific to the S type: m7, m8 and *yciR* 1063, four to the R type: m10-13, and three to the W type: m9, *bfr61*, and *wspE*. The two endemic S mutations consisted of m6, a

silent SNP in the succinate dehydrogenase (*sqr*) gene at position 441 on chromosome 2 and m7, a 49-gene deletion on chromosome 2 (Table 1). The m7 deletion eliminated several genes predicted to affect antibiotic resistance, including two *emrB/qacA* multi-drug resistance transporter genes (gene ID 639696629 and 639696639), penicillin binding protein 1C gene (*pbpC*) (gene ID 639696612), a fusaric acid resistance protein (gene ID 639696637), and a beta-lactamase gene (gene ID 639696655) (Table 4).

We confirmed four mutations unique to the R morphotype consisting of m10, m11, m12, and m13, with both the m10 and m11 genes having been previously identified to contribute to biofilm and motility characteristics in *Pseudomonas aeruginosa* CF lung infections (Smith, Buckley et al. 2006) (Table 1). The m10 mutation contained by the R type was found in gene position 103 in the *wspD* gene on chromosome 2. This gene is a member of the *wsp* operon, a signal transduction pathway responsible for altering levels of cyclic-di-GMP (D'Argenio, Calfee et al. 2002; D'Argenio and Miller 2004; McDonald, Gehrig et al. 2009). Interestingly, the m13 mutation in *wspA* and *wspE* found only in the W type is also a member of this operon. The m11 mutation occurred 90 base pairs 5' of an operon containing an aminoglycoside glycosyltransferase and is also a *P. aeruginosa* *rhIB* homolog (Jeannot, Elsen et al. 2008; Dubeau, Deziel et al. 2009). This enzyme is responsible for the production of rhamnolipids, which are surface-active molecules composed of rhamnose and  $\beta$ -hydroxydecanoic acid and act as

biosurfactants produced by *Burkholderia* spp. and *P. aeruginosa* (Boles, Thoendel et al. 2005; Dubeau, Deziel et al. 2009).

The m11 mutation specific to R occurred 18 base pairs 5' to the *mltA* gene on chromosome 1. This gene has been identified with six major lytic endotransglycosylase genes expressed in *E. coli* (Lommatzsch, Templin et al. 1997). The enzyme MltA cleaves  $\beta$ -1, 4 glycosidic bonds between the *N*-acetylglucosamine and *N*-acetylmuramic acid residues of peptidoglycan polymers, thereby catalyzing the intramolecular transglycosylation of the muramic acid residue producing 1,6-anhydro-muropeptides (Lommatzsch, Templin et al. 1997). Finally the m12 mutation is found in a conserved open reading frame annotated simply as DUF88 and is of unknown function.

The mutations shared by the three completely re-sequenced isolates were selected as candidates to screen among clones within and among genotypes and for a phylogenetic analysis of their haplotype relationships and relative abundance. These mutations were m2, m4, m6, m9, and a different bacterioferritin promoter mutation termed *bfr* 61 (mapping approximately to the -35 position of the transcriptional start site) that were identified by targeted sequencing of select isolates (Tables 2, 3, and 4) and confirmed by complete genome sequencing (Figure 1 and Table 5).

Allelic Frequency at 750 Generations					
Allele	S	R	W	All	
<b>yciR</b>	6/10	6/10	2/10	14/30	46.67%
<b>manC</b>	3/10	1/10	1/10	5/30	16.67%
<b>Bfr 37</b>	1/10	0/10	0/10	1/30	3.33%
<b>Bfr 61</b>	0/10	0/10	9/10	9/30	30.00%

**Table 2.** Frequencies of mutant alleles detected in S, R, and W (10 isolates per type) morphotypes at 750-generations. Note that the *yciR* deletion was prevalent relative to other mutations overall and the *bfr* 61 mutation dominated the W population (also see Figure 1).

Allelic Frequency at 1500 Generations					
Allele	S	R	W	All	
<b>yciR</b>	7/10	10/10	7/10	24/30	80.00%
<b>manC</b>	5/10	10/10	8/10	23/30	76.67%
<b>Bfr 37</b>	8/10	10/10	9/10	27/30	90.00%
<b>Bfr 61</b>	0/10	0/10	1/10	1/30	3.33%
<b>wspD</b>	0/10	10/10	0/10	10/30	33.3%

**Table 3.** Frequencies of mutant alleles detected in S, R, and W (10 isolates per type) morphotypes at 1500-generations. Note that the *yciR* deletion background increased in frequency and that the *bfr* 61 mutation had nearly

been replaced by the *bfr* 37 background. Also, the *wspD* mutation was found exclusively in R mutants between 750 and 1500-generations.

The <i>yciR</i> deletion evolves repeatedly in multiple populations			
Population	S	R	W
B 1	<i>yciR</i> -	<i>yciR</i> -	<i>yciR</i> -
B 2	WT	<i>yciR</i> -	<i>yciR</i> -
B 3	WT	<i>yciR</i> -	<i>yciR</i> -
B 4	<i>yciR</i> -	<i>yciR</i> -	WT
B 5	<i>yciR</i> -	<i>yciR</i> -	WT
B 6	<i>yciR</i> -	<i>yciR</i> -	WT

**Table 4.** Detection of the *yciR* gene deletion in replicate experimental biofilm populations after 1500-generations. The *yciR* deletion was detected in all biofilm populations, although not always S and W types.

Generation detected	450	1050	1500
Ferrochelatase	100.0%	100.0%	100.0%
2-oxoglutarate dehydrogenase ( <i>ogdh</i> )	16.7%	91.2%	97.5%
$\Delta$ near <i>lysR</i> regulator	11.3%	73.5%	86.0%
<i>wspA</i> 587	6.2%	ND	0.7%
<i>yciR</i> 1063	63.1%	ND	1-3%
monooxygenase, FAD-binding	54.5%	12.0%	
<i>yciR</i> 316	15.5%		
<i>rpoC</i> , RNA polymerase, beta subunit	12.2%		
extracellular solute-binding protein, family 5	5.4%		
Polyribonucleotide nucleotidyltransferase	4.6%		
hypothetical	4.3%		
amino acid permease-associated region	3.7%		
aspartate/aromatic aminotransferase	3.5%		
glycosyltransferase	2.7%		



type 2, 5' of <i>capD</i>		
<i>mscS</i>	93.2%	97.8%
<i>bfr 37</i>	84.0%	97.0%
<i>pvdA</i> of pyoverdinin biosynthesis	4.0%	3.0%
<i>bfr 61</i>	1.0%	3.0%
<i>lysR</i> transcriptional regulator	4.5%	1.7%
<i>manC</i> (SNP)	4.5%	
rhamnosyltransferase <i>wbgA</i>	2.9%	
probable Fe-S binding protein	2.7%	
ferric iron ABC transporter	2.2%	
ABC-type spermidine/putrescine transport system	2.2%	
3' of <i>araC</i>		
transcriptional regulator	2.1%	
$\Delta manC$		97.4%
succinate dehydrogenase ( <i>sqr</i> )		31.8%
DUF88		29.3%
<i>mltA</i>		25.0%
<i>wspD</i>		22.5%
<i>bfd</i> ferredoxin (2Fe 2S)		5.4%
<i>wspE</i>		4.6%
sugar transferase		3.5%
<i>wspA 1220</i>		W isolate
macroglobulin KO (49 genes)		S isolate
5' of <i>rhIB</i> operon		R isolate
		All
<i>yciR</i> KO (95 genes)		isolates

**Table 5.** All mutations detected from Illumina sequencing of population metagenomes and morphotype clones. Metagenome sequencing at 450, 1050, and 1500 generations demonstrates a high degree of population heterogeneity and turnover. Mutations highlighted in blue indicate those mutations that persisted through 1500 generations.

## Discussion

Microbial biofilm populations are typically characterized by high levels of physiological species heterogeneity in both the environment and chronic CF lung infections (Stewart and Franklin 2008); however, the mechanisms of adaptation to long-term biofilm selection is mostly unknown (Smith, Buckley et al. 2006). Here we examine the origin and fate of adaptive mutations occurring in a biofilm community that evolved for 1500 generations under controlled laboratory conditions (Poltak and Cooper 2010). We hypothesized that under this selective regime, mutations would arise in genes previously identified to play a role in biofilm formation. We also tracked the presence of several of these mutations to determine whether the sequenced clones were reflective of the true genetic diversity found in the population. Our analysis reveals that not only did several mutations occur in genes associated with biofilm production, which increased among all evolved mutants, but that evolved biofilm populations retained high genomic heterogeneity both within and among mutants adapted to distinct ecological niches.

These ecological niches are unique to each morphotype and are defined by their biofilm colonization and cross-feeding abilities. Specifically, the S type has been shown to be the weakest biofilm producer yet can attach

readily to polystyrene surfaces and on microcolonies of the W type as thin biofilm. It is able to cross-feed efficiently from its own secondary metabolites and those from R and W. The R type and the W type produce similar quantities of biofilm; however, R is usually found in dense microcolonies at the bead surface spreading horizontally and is not closely associated with either S or W. It is able to cross-feed on the secondary metabolites of S and W but cannot grow on its own secreted metabolites. The W type rapidly colonizes polystyrene surfaces as dense, tall microcolonies. W also acts as an attachment site for the S type and therefore increases the overall carrying capacity of the biofilm population in mixed culture. The S type also increases the cellular productivity of W in culture. W is also unable to grow on its own secondary metabolites but can grow on those from S and R extremely well. Therefore, the phenotypic differences between the morphotypes can facilitate the growth and attachment of each other.

**Experimental biofilm populations rapidly generate genomic heterogeneity that is purged by not always eliminated by selective sweeps**

Our previous work has shown that the biofilm selective environment facilitates the evolution and persistence of phenotypic heterogeneity so we predicted that the genomic diversity within these populations would be equally heterogeneous. However, we found not only is that genomic diversity was much more extensive than we predicted, but that the turnover of newly

detected mutations was rapid (Table 2). We speculate that this turnover was due to frequent, but incomplete selective sweeps carried out by a dominant genomic background that accumulated several beneficial mutations (Figure 1). Although we have not yet directly tested which of these mutations are adaptive in nature it is very likely that several mutations found in all three morphotypes are adaptive and that mutations unique to specific morphotypes (Table 1) are responsible for their phenotypic heterogeneity (Poltak and Cooper 2010). We also acknowledge that some mutations such as *mscS* (m4) and succinate dehydrogenase (*sqr*) (m8) may have risen to high frequency and persisted by genetic hitchhiking along with adaptive mutations.

The most significant selective sweep occurred in population B1 between 750 and 1500 generations with the fixation of the bacterioferritin promoter mutation m3 that allowed this background to take over the population by 97% (Table 1 and Figure 1). Interestingly, the m3 mutation was detected only in the S morphotype at 750 generations but later revolutionized the population by generating new R and W types by acquiring new mutations specific to morphotypes that allowed them to outcompete the resident W and R types for their established niches (Figure 1). We also found further support for the rapid increase of the *bfr37* mutation (m1) in the dominant lineage by detecting the presence or absence of m1 and other dominant alleles in multiple clones of each morphotype over time (Tables 2 and 3).

Aside from the dominant genomic background detected throughout the biofilm evolution, there were other genotypes that were able to rise to detectable frequencies (Table 2), with only six detected at multiple time points (Figure 1 and Table 2). Although we have not yet identified whether the multiple persistent mutations detected in population B1 are linked, it is likely that many if not all are directly connected (Figure 1). The coexistence of multiple genomic backgrounds arising from a single ancestor in biofilms is not unprecedented since a previous study found that *E. coli* biofilm populations in chemostats exhibit an apparent increased tolerance of genetic heterogeneity (Ponciano, La et al. 2009). We considered the possibility that these populations experienced conditions favoring elevated mutation rates, but this would have resulted in abnormally high levels of genetic diversity in all genome regions, not just replacement substitutions in coding regions. Hypermutability would also not explain the strong parallelism in mutations associated with adaptation (i.e. multiple alleles of *yciR* and *wspA*) among the different lineages within the population. We speculate that the ability for biofilm populations to maintain multiple adaptive lineages may be caused by the structure of the biofilm itself or by interactions among lineages that prevent the rapid purging seen in homogeneous planktonic populations (Rainey and Travisano 1998).

**Genes involved in iron metabolism were an underlying target in experimental biofilm adaption**

Due to the number of mutations that occurred in genes annotated as contributing to iron metabolism and the inherent lack of iron in our selective environment, the selective pressure on iron metabolism in general may have been high for all morphotypes. This is not surprising since iron has been shown to be an essential, although limited, resource in biofilms (Banin, Vasil et al. 2005) including those in chronic biofilm infections (Smith, Buckley et al. 2006). In addition, competition for this resource within biofilms has been shown to result in antagonistic and cooperative behaviors between community variants (Diggle, Griffin et al. 2007). Iron acquisition has also been determined to influence colony morphology *in vivo* (Chantratita, Wuthiekanun et al. 2007).

Our work suggests that bacterioferritin was a major target of selection due to the fact that two separate mutational events occurred in the promoter region of this gene. In addition several other genes related to iron metabolism were mutated or deleted (Table 6 and 7). Specifically, three genes involving iron metabolism were found in the 95-gene deletion where a ferredoxin (*bfd*) gene, a ferredoxin iron-sulfur binding protein as well as a Rieske iron-sulfur binding protein were included within the 95-gene deletion. Why so mutations occurred in iron utilization genes is unclear, however it is likely that competition for iron and the accumulation of mutations in these genes may be a result of the iron-limiting conditions of our system. Our assay of intracellular iron concentrations confirmed that all three morphotypes exhibited

significantly reduced stored iron relative to the ancestral genotype, which may be directly correlated to one or more of the mutations found in genes related to iron metabolism (Figure 2).

### **Experimental biofilm evolution favors mutations known to influence biofilm production as well as those found in chronic infections**

Several mutations occurred in genes previously found mutated in chronic infections (Hickman, Tifrea et al. 2005; Smith, Buckley et al. 2006). Notably, four mutations were detected in genes within the *wsp* (wrinkly spreader phenotype) operon (D'Argenio, Calfee et al. 2002; Goymer, Kahn et al. 2006; Guvener and Harwood 2007) in the R or W type. One R type mutation occurred 5' to *rhIB*, a gene responsible for rhamnolipid production (Dubeau, Deziel et al. 2009) and critical in the formation of biofilm channels, detachment, and motility in both *Burkholderia* spp. and *P. aeruginosa* (Boles, Thoendel et al. 2005; Dubeau, Deziel et al. 2009). Although we do not know the exact effects of these mutations, it is known that mutations in the *wsp* operon may generate the wrinkly phenotype seen in CF lung isolates of *Burkholderia* spp. and *P. aeruginosa* (D'Argenio, Calfee et al. 2002) and that the *wspD* may be responsible for the ruffled spreader colony morphology. Also, these colony morphologies are commonly collected from CF patient sputum samples (Haussler, Lehmann et al. 2003; Haussler, Ziegler et al. 2003; Chantratita, Wuthiekanun et al. 2007) suggesting that the selective pressures promoting biofilm forming specialists may be simply result from

selection for adherent cell types and be less specific to the lung environment itself.

The mutations detected in population B1 involved in biofilm formation are found in the *manC* gene (m4), and *yciR* (m2). The *manC* mutation may directly alter the function of the gene and production of the exopolysaccharide cepacian in all morphotypes (Sist, Cescutti et al. 2003). The truncation of this gene suggests that the catabolic domain of *manC* that allows the conversion of mannose-1-phosphate to D-mannose may be rendered inactive by its premature stop. This evolved protein is likely now solely focused on anabolism and no longer on catabolism, thus increasing production of key biofilm substrates. The *yciR* deletion may have significant regulatory effects on the *cepI*R quorum sensing system and on c-di-GMP production that influence biofilm formation (Huber, Riedel et al. 2002). We speculate that this mutation was critical in the adaptation to our biofilm selection model since two separate mutations occurred early (450 generations) in the experiment. Although it is likely that the loss of this regulatory gene may cause the constitutive expression of genes that promote biofilm production, we have not concluded the actual effect of each *yciR* mutation.

**Niche-specific adaptation in the biofilm requires few mutations and may be recurrent**



Several mutations detected in our analysis were found only in certain morphotypes and are likely related to their niche specificity. Specifically it is likely that a mutation within the *wspA* gene is capable of generating a wrinkly colony morphotype that overproduces biofilm, limits planktonic growth but improves fitness relative to the ancestor in colonizing the bead. In addition, a *wspD* mutation is found exclusively in the R type and therefore may be responsible for the spreading phenotype and increased biofilm production and fitness. The R clone also carries three other mutations that potentially pertain to its characteristics as a biofilm specialist, including one that may alter rhamnolipid production and another (*mltA*) that likely influences cell wall peptidoglycan biosynthesis (Table 1). The S clone only carries two unique mutations, one silent and the other consisting of a 49-gene deletion that may have multiple effects on the phenotypic profile of this morphotype. This deletion is of particular interest since the deletion contains several genes annotated as being related to antibiotic resistance (Table 7). Initially we suspected that this deletion could involve a potential pathogenicity island conferring antibiotic resistance, however there are no transposases adjacent to this deletion that would support this idea.

Due to the spatial structure of a biofilm, multiple lineages may coexist neutrally because interactions may be minimized, but also adaptation to the biofilm may itself generate multiple microniches. This potential increase in niche availability may explain why multiple biofilm variants or genotypes

emerge and persist. This scenario allows selection to act in two separate dimensions. First, selection will act upon the population as a whole where it will select those genotypes most fit to the environment. Second, selection will act at the microniche level where competitive exclusion acts locally. Taking both dimensions into account, the persistence of multiple genomic backgrounds becomes likely, since different adaptive mutations may confer similar fitness within a given niche existing in multiple locations. For example, the W morphotype evolved by at least two different mutations in the *wsp* operon on different genomic backgrounds (Figure 1 and Tables 1 and 5). This may be the case as well for R since it was found both before and after the rise of the *bfr* (m6) mutation. (Figure 1 and Tables 1 and 5). Finally, we acknowledge that the independent function and contribution of each of these mutations remains to be confirmed and we have yet to identify most of the adaptive mutations in the other populations.

**Table 6.** 95-gene deletion (m2) on chromosome 2, nucleotide positions 397098 to 494098 found in all three morphotypes.

IMG id	
639695613	<i>yciR</i> diguanylate cyclase/phosphodiesterase with PAS/PAC sensor(s)
639695614	Enoyl-CoA hydratase/isomerase
639695615	hypothetical protein
639695616	conserved hypothetical protein
639695617	hypothetical protein
639695618	transcriptional regulator, AraC family
639695619	major facilitator superfamily MFS_1
639695620	aldo/keto reductase
639695621	transcriptional regulator, LysR family

639695622 PEP phosphonmutase  
639695623 transcriptional regulator, MarR family  
639695624 conserved hypothetical protein  
639695625 Glutathione S-transferase, C-terminal domain  
639695626 HAD-superfamily hydrolase, subfamily IA, variant 1  
639695627 Ornithine cyclodeaminase  
639695628 alanine racemase domain protein  
639695629 transcriptional regulator, LysR family  
639695630 FAD-dependent pyridine nucleotide-disulphide oxidoreductase  
639695631 transcriptional regulator, BadM/Rrf2 family  
639695632 conserved hypothetical protein  
639695633 molecular chaperone-like  
639695634 molecular chaperone-like  
639695635 amidinotransferase  
639695636 Ornithine cyclodeaminase  
639695637 transcriptional regulator, AsnC family  
639695638 uncharacterized peroxidase-related enzyme  
639695639 conserved hypothetical protein  
639695640 monooxygenase, FAD-binding  
639695641 transcriptional regulator, LysR family  
639695642 Extracellular ligand-binding receptor  
639695643 inner-membrane translocator  
639695644 ABC transporter related  
639695645 ABC transporter related  
639695646 conserved hypothetical protein  
639695647 periplasmic sensor signal transduction histidine kinase  
639695648 two component transcriptional regulator, winged helix family  
639695649 ABC nitrate/sulfonate/bicarbonate transporter, periplasmic ligan  
639695650 major facilitator superfamily MFS\_1  
639695651 conserved hypothetical protein  
639695652 plasmid stabilization system  
639695653 periplasmic sensor signal transduction histidine kinase  
639695654 two component transcriptional regulator, LuxR family  
639695655 conserved hypothetical protein  
639695656 DedA family membrane protein  
639695657 putative transcriptional regulator  
639695658 protein of unknown function DUF891  
639695659 Alpha/beta hydrolase fold-3 domain protein  
639695660 glucose-methanol-choline oxidoreductase  
639695661 transcriptional regulator, AraC family  
639695662 GCN5-related N-acetyltransferase  
639695663 conserved hypothetical protein  
639695664 conserved hypothetical protein

639695665 transcriptional regulator, AsnC family  
639695666 protein of unknown function DUF1234  
639695667 major facilitator superfamily MFS\_1  
639695668 4-hydroxyphenylacetate 3-monooxygenase, reductase subunit  
639695669 two component transcriptional regulator, LuxR family  
639695670 short-chain dehydrogenase/reductase SDR  
639695671 Amidase  
639695672 conserved hypothetical protein  
639695673 conserved hypothetical protein  
639695674 Acyl-CoA dehydrogenase, type 2, C-terminal domain  
639695675 PAS/PAC sensor signal transduction histidine kinase  
639695676 4-oxalocrotonate tautomerase family enzyme  
639695677 aromatic-ring-hydroxylating dioxygenase, beta subunit  
639695678 Rieske [2Fe-2S] domain protein  
639695679 transcriptional regulator, LysR family  
639695680 ferredoxin  
639695681 major facilitator superfamily MFS\_1  
639695682 porin, Gram-negative type  
639695683 transcriptional regulator, LysR family  
639695684 transcriptional regulator, AraC family  
639695685 NAD/NADP octopine/nopaline dehydrogenase  
639695686 3-hydroxyacyl-CoA dehydrogenase, NAD-binding  
639695687 major facilitator superfamily MFS\_1  
639695688 extracellular solute-binding protein, family 1  
639695689 FAD dependent oxidoreductase  
639695690 Ferredoxin domain protein [2Fe-2S]-binding domain protein  
639695691 conserved hypothetical protein  
639695692 binding-protein-dependent transport systems inner membrane componet  
639695693 binding-protein-dependent transport systems inner membrane componet  
639695694 ABC transporter related  
639695695 hypothetical protein  
640068494 transcriptional regulator, IclR family  
639695696 short-chain dehydrogenase/reductase SDR  
639695697 Twin-arginine translocation pathway signal  
639695698 conserved hypothetical protein  
639695699 transcriptional regulator, AraC family  
639695700 GCN5-related N-acetyltransferase  
639695701 conserved hypothetical protein  
639695702 transcriptional regulator, XRE family  
639695703 3-beta hydroxysteroid dehydrogenase/isomerase  
639695704 Alcohol dehydrogenase, zinc-binding domain protein  
639695704 transcriptional regulator, LysR family  
639695705 FAD-dependent pyridine nucleotide-disulphide oxidoreductase

639695706 **End Deletion**  
 transposase IS116/IS110/IS902 family protein  
 639695707

**Table 7.** 46-gene deletion from chromosome 2 found in the S1500 clone (m7), nucleotide positions 1517098 to 1576098.

IMG ID	S-type deletion 2
639696611	alpha-2-macroglobulin domain protein; extracellular alpha helices
639696612	<b>TIGRFAM: penicillin-binding protein 1C; PbpC, transglycosylase, membrane biogenesis</b>
639696613	SPTR: Q1BNV2 Hypothetical protein. Burkholderia cenocepacia AU 1054.
639696614	SPTR: Q1BNV3 Hypothetical protein precursor. Burkholderia cenocepacia AU 1054.
639696615	PFAM: GCN5-related N-acetyltransferase
639696616	PFAM: major facilitator superfamily MFS_1
639696617	SPTR: Q1BNV6 Hypothetical protein precursor. Burkholderia cenocepacia AU 1054.
639696618	glutamate/aspartate binding precursor gltI
639696619	PFAM: peptidase S8 and S53, subtilisin, kexin, sedolisin
639696620	SPTR: Q1BNV9 Hypothetical protein precursor. Burkholderia cenocepacia AU 1054.
639696621	TIGRFAM: ATPase, P-type (transporting), HAD superfamily, subfamily IC
639696622	SPTR: Q4LJB6 Hypothetical protein. Burkholderia cenocepacia HI2424.
639696623	PFAM: regulatory protein, LysR; LysR, substrate-binding
639696624	SPTR: Q1BNW3 Hypothetical protein. Burkholderia cenocepacia AU 1054.
639696625	PFAM: peptidase S11, D-alanyl-D-alanine carboxypeptidase 1; peptidoglycan biosynthesis
639696626	SPTR: Q1BNW5 Hypothetical protein. Burkholderia cenocepacia AU 1054.
639696627	PFAM: regulatory protein, MarR
639696628	PFAM: isochorismatase hydrolase
639696629	<b>TIGRFAM: drug resistance transporter, EmrB/QacA subfamily</b>
639696630	SPTR: Q4LJC4 Lysine exporter protein (LYSE/YGGA). Burkholderia cenocepacia HI2424.
639696631	PFAM: regulatory protein, LysR; LysR, substrate-binding
639696632	PFAM: Sulfate transporter/antisigma-factor antagonist STAS; sulphate transporter
639696633	PFAM: MscS Mechanosensitive ion channel
639696634	PFAM: regulatory protein GntR, HTH; aminotransferase, class I and II

639696635 TIGRFAM: oxidoreductase alpha (molybdopterin) subunit

639696636 PFAM: protein of unknown function UPF0187

639696637 **PFAM: Fusaric acid resistance protein conserved region**

639696638 PFAM: regulatory protein, LysR; LysR, substrate-binding

639696639 **TIGRFAM: drug resistance transporter, EmrB/QacA subfamily**

639696640 SPTR: Q1BNX9 Hypothetical protein precursor. Burkholderia cenocepacia AU 1054.

639696641 PFAM: extracellular solute-binding protein, family 5, peptide/nickel transport

639696642 SPTR: Q1BNY1 Hypothetical protein. Burkholderia cenocepacia AU 1054.

639696643 **TIGRFAM: Mn<sup>2+</sup>/Fe<sup>2+</sup> transporter, NRAMP family; mnTH, manganese transport protein**

639696644 oxalate decarboxylase (glyoxylate shunt), converts oxalate to formate

639696645 SPTR: Q1BNY4 Putative transcriptional regulator, RpiR family.

639696646 PFAM: peptidase M15D, vanX D-ala-D-ala dipeptidase; VanY/endolysins

639696647 PFAM: extracellular solute-binding protein, family 5

639696648 PFAM: binding-protein-dependent transport systems inner membrane component

639696649 PFAM: binding-protein-dependent transport systems inner membrane component

639696650 PFAM: ABC transporter related

639696651 PFAM: ABC transporter related

639696652 PFAM: Transglycosylase-associated protein

639696653 SPTR: Q1BNZ2 Hypothetical protein precursor. Burkholderia cenocepacia AU 1054.

639696654 PFAM: regulatory protein, LysR; LysR, substrate-binding

639696655 **PRIAM: Beta-lactamase**

639696656 PFAM: Peptidoglycan-binding LysM; peptidase M23B

639696657 PFAM: regulatory protein, LysR; LysR, substrate-binding

639696658 PFAM: protein of unknown function DUF1486

639696659 Hypothetical signal peptide

## Conclusion

We have presented one of the first experimental evolution projects using *Burkholderia*, a genus with exceptional functional diversity and pervasiveness in biofilm associated environments and hosts (Mahenthiralingam, Urban et al. 2005). Several *Burkholderia* species are found infecting the lungs of cystic fibrosis (CF) patients (Haussler, Lehmann et al. 2003; Mahenthiralingam, Urban et al. 2005), causing chronic biofilm infections that are often fatal (Mahenthiralingam et al. 2005). Like the more common CF lung pathogen, *Pseudomonas aeruginosa*, *Burkholderia* chronic lung infections generate detectable biofilm population diversity characterized by increased variable colony morphology, biofilm production, antimicrobial resistance, and mortality (Haussler et al. 2003; Haussler et al. 2003; Nguyen and Singh 2006; Chantratita et al. 2007). Therefore, it has been our goal to identify both the ecological and evolutionary mechanisms that underlie chronic biofilm adaptation.

In order to study biofilm adaption we developed a novel biofilm experimental model that was able to maintain all replicate populations over five months and could continue indefinitely to mimic the scale of prolonged chronic infections. This system has also enabled mechanistic study of the evolution and maintenance of biofilm diversity. Initially, we examined the relationship between diversity and productivity, an association that has

remained uncertain due to several antagonistic and positive interactions that may occur in complex communities. By quantifying the biofilm cellular productivity of evolved morphotypes cultured alone and as mixed populations we found that productivity was optimal in mixture. Furthermore, we confirmed that biofilm diversification was driven by competition or availability for resources and space, however we also found that facilitation by the sequential construction of new niches played a critical role. Specifically, we identified that the incidental production of metabolic byproducts varied among biofilm variants enabling each type to cross-feed from one another. In addition, we identified the production of new structures that promoted the adherence of other types. These findings may help explain the role of diversity not only in structured microbial communities but also in a wide range of complex natural ecosystems. Alternatively, by understanding how different species facilitate the growth of others within pathogenic biofilms we may be able to prevent adaptation and progression of chronic CF lung infections. (Haussler et al. 2003; Haussler et al. 2003; Boles et al. 2004; Nguyen and Singh 2006; Smith et al. 2006).

Finally, we hypothesized that under biofilm selective conditions, mutations in pathways known to be important in biofilm production such as exopolysaccharide production (Sist et al. 2003) and c-di-GMP (Hengge 2009) would be favored. To test this hypothesis, we obtained and compared the complete genome sequences of clones of each of three distinct colony



morphotypes, studded (S) type, ruffled (R), and wrinkly (W), to the ancestral genotype, *B. cenocepacia* strain HI2424 (Coenye et al. 2004; Poltak and Cooper 2010). In collaboration with the Joint Genome Institute (JGI), we also obtained metagenome sequences from samples of the mixed population in which these clones evolved at three evolutionary time points. These genome and population sequences identified many critical mutations associated with adaptation and enabled us to reconstruct the evolutionary history of adaptation and diversification in a single biofilm population.

In conclusion, we hope to further characterize the behavior of all adapted biofilm genotypes and the function of each mutation found in our focal population. In addition, we intend to identify the adaptive mutations in our replicate populations to examine potential ecological and evolutionary parallelism. Finally, although the natural environment and the CF lung are much more complex than our controlled model system, we have observed mutations in *Burkholderia cenocepacia in vitro* that are in the same or related genes in *P. aeruginosa in vivo* from the CF lung. This intriguing finding suggests that if the underlying molecular targets of biofilm adaptation are conserved among species, then biofilm adaptation may follow a common evolutionary path in many biofilm associated environments and hosts.

## LIST OF REFERENCES

- Andrews, S. C., P. M. Harrison, et al. (1989). "Cloning, sequencing, and mapping of the bacterioferritin gene (bfr) of Escherichia coli K-12." J Bacteriol **171**(7): 3940-3947.
- Banin, E., M. L. Vasil, et al. (2005). "Iron and Pseudomonas aeruginosa biofilm formation." Proc Natl Acad Sci U S A **102**(31): 11076-11081.
- Barrick, J. E., D. S. Yu, et al. (2009). "Genome evolution and adaptation in a long-term experiment with Escherichia coli." Nature **461**(7268): 1243-1247.
- Beaumont, H. J., J. Gallie, et al. (2009). "Experimental evolution of bet hedging." Nature **462**(7269): 90-93.
- Bertness, M. D. and S. W. Shumway (1993). "Competition and facilitation in marsh plants." Am Nat **142**(4): 718-724.
- Boles, B. R., M. Thoendel, et al. (2004). "Self-generated diversity produces "insurance effects" in biofilm communities." Proc Natl Acad Sci U S A **101**(47): 16630-16635.
- Boles, B. R., M. Thoendel, et al. (2005). "Rhamnolipids mediate detachment of Pseudomonas aeruginosa from biofilms." Mol Microbiol **57**(5): 1210-1223.
- Brockhurst, M. A. (2007). "Population bottlenecks promote cooperation in bacterial biofilms." PLoS ONE: e634.
- Brockhurst, M. A., A. Buckling, et al. (2007). "Cooperation peaks at intermediate disturbance." Curr Biol **17**(9): 761-765.
- Brockhurst, M. A., M. E. Hochberg, et al. (2006). "Character displacement promotes cooperation in bacterial biofilms." Curr Biol **16**(20): 2030-2034.
- Bruschi, M. and F. Guerlesquin (1988). "Structure, function and evolution of bacterial ferredoxins." FEMS Microbiol Rev **4**(2): 155-175.
- Buckling, A. and P. B. Rainey (2002). "The role of parasites in sympatric and allopatric host diversification." Nature **420**(6915): 496-499.

- Bull, J. J. and W. R. Harcombe (2009). "Population dynamics constrain the cooperative evolution of cross-feeding." PLoS One **4**(1): e4115.
- Cardinale, B. J., J. P. Wright, et al. (2007). "Impacts of plant diversity on biomass production increase through time because of species complementarity." Proceedings of the National Academy of Sciences **104**(46): 18123-18128.
- Chantratita, N., V. Wuthiekanun, et al. (2007). "Biological relevance of colony morphology and phenotypic switching by *Burkholderia pseudomallei*." J Bacteriol **189**(3): 807-817.
- Coenye, T., T. Spilker, et al. (2004). "Recovery of *Burkholderia cenocepacia* strain PHDC from cystic fibrosis patients in Europe." Thorax **59**(11): 952-954.
- Connell, J. H. and R. O. Slatyer (1977). "Mechanisms of succession in natural communities and their role in community stability and organization." The American Naturalist **111**(982): 1119-1144.
- Cooper, V. S. and R. E. Lenski (2000). "The population genetics of ecological specialization in evolving *Escherichia coli* populations." Nature **407**(6805): 736-739.
- Costerton, J. W. (2001). "Cystic fibrosis pathogenesis and the role of biofilms in persistent infection." Trends in Microbiology **9**(2): 50-52.
- D'Argenio, D. A., M. W. Calfee, et al. (2002). "Autolysis and autoaggregation in *Pseudomonas aeruginosa* colony morphology mutants." J Bacteriol **184**(23): 6481-6489.
- D'Argenio, D. A. and S. I. Miller (2004). "Cyclic di-GMP as a bacterial second messenger." Microbiology **150**(Pt 8): 2497-2502.
- Davey, M. E. and A. O'Toole G (2000). "Microbial biofilms: from ecology to molecular genetics." Microbiol Mol Biol Rev **64**(4): 847-867.
- Davies, D. G. and G. G. Geesey (1995). "Regulation of the alginate biosynthesis gene *algC* in *Pseudomonas aeruginosa* during biofilm development in continuous culture." Appl Environ Microbiol **61**(3): 860-867.

- Davis, G. D., C. Elisee, et al. (1999). "New fusion protein systems designed to give soluble expression in *Escherichia coli*." *Biotechnol Bioeng* **65**(4): 382-388.
- Day, T. (2004). "Competitive and facilitative evolutionary diversification." *BioScience* **54**(2): 101-109.
- Day, T. and K. A. Young (2004). "Competitive and Facilitative Evolutionary Diversification." *BioScience* **54**(2): 101-109.
- Diggle, S. P., A. S. Griffin, et al. (2007). "Cooperation and conflict in quorum-sensing bacterial populations." *Nature* **450**(7168): 411-414.
- Doebeli, M. (2002). "A model for evolutionary dynamics of cross-feeding polymorphisms in microorganisms." *Population Ecology* **44**: 59-70.
- Dubeau, D., E. Deziel, et al. (2009). "*Burkholderia thailandensis* harbors two identical *rhl* gene clusters responsible for the biosynthesis of rhamnolipids." *BMC Microbiol* **9**: 263.
- Elena, S. F. and R. E. Lenski (2003). "Evolution experiments with microorganisms: the dynamics and genetic bases of adaptation." *Nat Rev Genet* **4**(6): 457-469.
- Ellis, C. N. and V. S. Cooper (2010). "Experimental adaptation of *Burkholderia cenocepacia* to onion medium reduces host range." *Appl Environ Microbiol*.
- Geritz, S. A. (2005). "Resident-invader dynamics and the coexistence of similar strategies." *J Math Biol* **50**(1): 67-82.
- Gottesman, S. and V. Stout (1991). "Regulation of capsular polysaccharide synthesis in *Escherichia coli* K12." *Mol Microbiol* **5**(7): 1599-1606.
- Goymer, P., S. G. Kahn, et al. (2006). "Adaptive divergence in experimental populations of *Pseudomonas fluorescens*. II. Role of the GGDEF regulator WspR in evolution and development of the wrinkly spreader phenotype." *Genetics* **173**(2): 515-526.
- Gross, K. and B. J. Cardinale (2007). "Does species richness drive community production or vice versa? Reconciling historical and contemporary paradigms in competitive communities." *Am Nat* **170**(2): 207-220.

- Guvener, Z. T. and C. S. Harwood (2007). "Subcellular location characteristics of the *Pseudomonas aeruginosa* GGDEF protein, WspR, indicate that it produces cyclic-di-GMP in response to growth on surfaces." Mol Microbiol **66**(6): 1459-1473.
- Habets, M. G., D. E. Rozen, et al. (2006). "The effect of population structure on the adaptive radiation of microbial populations evolving in spatially structured environments." Ecol Lett **9**(9): 1041-1048.
- Hall-Stoodley, L., J. W. Costerton, et al. (2004). "Bacterial biofilms: from the natural environment to infectious diseases." Nat Rev Microbiol **2**(2): 95-108.
- Hansen, S. K., P. B. Rainey, et al. (2007). "Evolution of species interactions in a biofilm community." Nature **445**(7127): 533-536.
- Harrison, F. and A. Buckling (2009). "Siderophore production and biofilm formation as linked social traits." ISME J **3**(5): 632-634.
- Haussler, S., C. Lehmann, et al. (2003). "Fatal outcome of lung transplantation in cystic fibrosis patients due to small-colony variants of the *Burkholderia cepacia* complex." Eur J Clin Microbiol Infect Dis **22**(4): 249-253.
- Haussler, S., I. Ziegler, et al. (2003). "Highly adherent small-colony variants of *Pseudomonas aeruginosa* in cystic fibrosis lung infection." J Med Microbiol **52**(Pt 4): 295-301.
- Hengge, R. (2009). "Principles of c-di-GMP signalling in bacteria." Nat Rev Microbiol **7**(4): 263-273.
- Hickman, J. W., D. F. Tifrea, et al. (2005). "A chemosensory system that regulates biofilm formation through modulation of cyclic diguanylate levels." Proc Natl Acad Sci U S A **102**(40): 14422-14427.
- Huang, L. N., H. De Wever, et al. (2008). "Diverse and distinct bacterial communities induced biofilm fouling in membrane bioreactors operated under different conditions." Environmental Science & Technology **42**(22): 8360-8366.
- Huber, B., K. Riedel, et al. (2002). "Genetic analysis of functions involved in the late stages of biofilm development in *Burkholderia cepacia* H111." Mol Microbiol **46**(2): 411-426.

- Hutchinson, G. (1957). "Concluding remarks." Cold Spring Harbor Symposium on Quantitative Biology **22**: 415-427.
- Jeannot, K., S. Elsen, et al. (2008). "Resistance and virulence of *Pseudomonas aeruginosa* clinical strains overproducing the MexCD-OprJ efflux pump." Antimicrob Agents Chemother **52**(7): 2455-2462.
- Jensen, S. O. and P. R. Reeves (2001). "Molecular evolution of the GDP-mannose pathway genes (*manB* and *manC*) in *Salmonella enterica*." Microbiology **147**(Pt 3): 599-610.
- Jones C.G., L. J. H., Shachak M. (1997). "Positive and negative effects of organisms as ecosystem engineers." Ecology **78**: 1946-1957.
- Korona, R., C. H. Nakatsu, et al. (1994). "Evidence for multiple adaptive peaks from populations of bacteria evolving in a structured habitat." Proc Natl Acad Sci U S A **91**(19): 9037-9041.
- Kovach, M. E., P. H. Elzer, et al. (1995). "4 New Derivatives of the Broad-Host-Range Cloning Vector P<sub>bbr1</sub>mcs, Carrying Different Antibiotic-Resistance Cassettes." Gene **166**(1): 175-176.
- Kreft, J. U. (2004). "Biofilms promote altruism." Microbiology **150**(Pt 8): 2751-2760.
- Kumar, S., M. Nei, et al. (2008). "MEGA: a biologist-centric software for evolutionary analysis of DNA and protein sequences." Brief Bioinform **9**(4): 299-306.
- Kuramitsu, H. K., X. He, et al. (2007). "Interspecies interactions within oral microbial communities." Microbiol Mol Biol Rev **71**(4): 653-670.
- Lambertsen, L., C. Sternberg, et al. (2004). "Mini-Tn7 transposons for site-specific tagging of bacteria with fluorescent proteins." Environmental Microbiology **6**(7): 726-732.
- Lenski, R. E. (1991). "Quantifying fitness and gene stability in microorganisms." Biotechnology **15**: 173-192.
- Li, H., J. Ruan, et al. (2008). "Mapping short DNA sequencing reads and calling variants using mapping quality scores." Genome Res **18**(11): 1851-1858.
- LiPuma, J. J., T. Spilker, et al. (2002). "An epidemic *Burkholderia cepacia* complex strain identified in soil." Lancet **359**(9322): 2002-2003.

- Lommatzsch, J., M. F. Templin, et al. (1997). "Outer membrane localization of murein hydrolases: MltA, a third lipoprotein lytic transglycosylase in *Escherichia coli*." J Bacteriol **179**(17): 5465-5470.
- Loreau, M. and A. Hector (2001). "Partitioning selection and complementarity in biodiversity experiments." Nature **412**(6842): 72-76.
- Lyautey, E., C. Jackson, et al. (2005). "Bacterial Community Succession in Natural River Biofilm Assemblages." Microbial Ecology **50**(4): 589-601.
- Mahenthiralingam, E., T. A. Urban, et al. (2005). "The multifarious, multireplicon *Burkholderia cepacia* complex." Nat Rev Microbiol **3**(2): 144-156.
- McDonald, M. J., S. M. Gehrig, et al. (2009). "Adaptive divergence in experimental populations of *Pseudomonas fluorescens*. IV. Genetic constraints guide evolutionary trajectories in a parallel adaptive radiation." Genetics **183**(3): 1041-1053.
- Meyer, J. R. and R. Kassen (2007). "The effects of competition and predation on diversification in a model adaptive radiation." Nature **446**(7134): 432-435.
- Miller, S., Dykes, D., Polesky, H. (1988). "A simple salting out method for extracting DNA from human nucleotide cells." Nucleic Acids Res **16**(4): 1215-1219.
- Nadell, C. D., J. B. Xavier, et al. (2009). "The sociobiology of biofilms." FEMS Microbiol Rev **33**(1): 206-224.
- Nagylaki, T. (1992). "Rate of evolution of a quantitative character." Proc Natl Acad Sci U S A **89**(17): 8121-8124.
- Nguyen, D. and P. K. Singh (2006). "Evolving stealth: genetic adaptation of *Pseudomonas aeruginosa* during cystic fibrosis infections." Proc Natl Acad Sci U S A **103**(22): 8305-8306.
- Nocker, A., J. E. Lepo, et al. (2004). "Influence of an oyster reef on development of the microbial heterotrophic community of an estuarine biofilm." Appl Environ Microbiol **70**(11): 6834-6845.
- O'Toole, G. A., L. A. Pratt, et al. (1999). "Genetic approaches to study of biofilms." Methods in Enzymology **310**: 91-109.

- Odling-Smee, F. J., K. N. Laland, et al. (2003). Niche construction: the neglected process in evolution. Princeton, NJ, Princeton University Press.
- Odling-Smee, L., and Feldman (2003). Niche Construction: the neglected process in evolution. Princeton, Princeton University Press.
- Odum, E. P. (1975). Ecology, Second Edition. New York, Holt, Rinehart, and Winston.
- P.E. Turner, V. S., RE Lenski (1996). "Tests of ecological mechanisms promoting the stable coexistence of two bacterial genotypes " Ecology **77**: 2119-2129.
- Palmer, K. L., L. M. Mashburn, et al. (2005). "Cystic fibrosis sputum supports growth and cues key aspects of *Pseudomonas aeruginosa* physiology." J Bacteriol **187**(15): 5267-5277.
- Palmer, R. J., Jr., K. Kazmerzak, et al. (2001). "Mutualism versus independence: strategies of mixed-species oral biofilms in vitro using saliva as the sole nutrient source." Infect Immun **69**(9): 5794-5804.
- Parke, J. L. and D. Gurian-Sherman (2001). "Diversity of the *Burkholderia cepacia* complex and implications for risk assessment of biological control strains." Annu Rev Phytopathol **39**: 225-258.
- Poltak, S., Cooper, V. (submitted 2010). "Ecological succession in long-term experimentally evolved biofilms produces synergistic communities." ISME J.
- Ponciano, J. M., H. J. La, et al. (2009). "Evolution of diversity in spatially structured *Escherichia coli* populations." Appl Environ Microbiol **75**(19): 6047-6054.
- Price, G. R. (1970). "Selection and covariance." Nature **227**(5257): 520-521.
- Rainey, P. B., A. Buckling, et al. (2000). "The emergence and maintenance of diversity: insights from experimental bacterial populations." Trends Ecol Evol **15**(6): 243-247.
- Rainey, P. B. and K. Rainey (2003). "Evolution of cooperation and conflict in experimental bacterial populations." Nature **425**(6953): 72-74.



- Rainey, P. B. and M. Travisano (1998). "Adaptive radiation in a heterogeneous environment." Nature **394**(6688): 69-72.
- Rakhimova, E., A. Munder, et al. (2008). "Fitness of Isogenic Colony Morphology Variants of *Pseudomonas aeruginosa* in Murine Airway Infection." PLoS ONE **3**(2): e1685.
- Ramette, A., J. J. LiPuma, et al. (2005). "Species abundance and diversity of *Burkholderia cepacia* complex in the environment." Appl Environ Microbiol **71**(3): 1193-1201.
- Ross-Gillespie, A., A. Gardner, et al. (2009). "Density dependence and cooperation: theory and a test with bacteria." Evolution **63**(9): 2315-2325.
- Rosenschweig, M. (1978). "Competitive speciation." Biological Journal of the Linnean Society **10**: 275-289.
- Rozen, D. E., P. J. Nadège, et al. (2009). "Death and cannibalism in a seasonal environment facilitate bacterial coexistence." Ecology Letters **12**(1): 34-44.
- Ruan, J., H. Li, et al. (2008). "TreeFam: 2008 Update." Nucleic Acids Res **36**(Database issue): D735-740.
- Singh, P. K., A. L. Schaefer, et al. (2000). "Quorum-sensing signals indicate that cystic fibrosis lungs are infected with bacterial biofilms." Nature **407**(6805): 762-764.
- Sist, P., P. Cescutti, et al. (2003). "Macromolecular and solution properties of Cepacian: the exopolysaccharide produced by a strain of *Burkholderia cepacia* isolated from a cystic fibrosis patient." Carbohydr Res **338**(18): 1861-1867.
- Smith, E. E., D. G. Buckley, et al. (2006). "Genetic adaptation by *Pseudomonas aeruginosa* to the airways of cystic fibrosis patients." Proc Natl Acad Sci U S A **103**(22): 8487-8492.
- Spencer, C., Saxer, G., Travisano, M., and M. Doebeli (2007). "Seasonal resource oscillations maintain diversity in bacterial microcosms." Evolutionary Ecology Research **9**: 775-787.
- Stachowicz, J. J. (2001). "Mutualism, facilitation, and the structure of ecological communities." BioScience **51**(3): 235-246.

- Starkey, M., J. H. Hickman, et al. (2009). "Pseudomonas aeruginosa rugose small colony variants have adaptations likely to promote persistence in the cystic fibrosis lung." J. Bacteriol.: JB.00119-00109.
- Stewart, P. S. and M. J. Franklin (2008). "Physiological heterogeneity in biofilms." Nat Rev Microbiol **6**(3): 199-210.
- Stoodley, P., K. Sauer, et al. (2002). "Biofilms as complex differentiated communities." Annu Rev Microbiol **56**: 187-209.
- Tamarit, J., V. Irazusta, et al. (2006). "Colorimetric assay for the quantitation of iron in yeast." Anal Biochem **351**(1): 149-151.
- Thomas, V. C., Y. Hiromasa, et al. (2009). "A fratricidal mechanism is responsible for eDNA release and contributes to biofilm development of Enterococcus faecalis." Mol Microbiol **72**(4): 1022-1036.
- Tsugita, A. and J. Yariv (1985). "Preliminary results for the primary structure of bacterioferritin of Escherichia coli." Biochem J **231**(1): 209-212.
- Turner, P. E., Souza, V., Lenski, RE (1996). "Tests of ecological mechanisms promoting the stable coexistence of two bacterial genotypes " Ecology **77**: 2119-2129.
- Velicer, G. J., G. Raddatz, et al. (2006). "Comprehensive mutation identification in an evolved bacterial cooperators and its cheating ancestor." Proc Natl Acad Sci U S A **103**(21): 8107-8112.
- Wright, P. F., S. Ankrah, et al. (2008). "Evaluation of the Langkat/dengue 4 chimeric virus as a live attenuated tick-borne encephalitis vaccine for safety and immunogenicity in healthy adult volunteers." Vaccine **26**(7): 882-890.
- Xavier, J. B. and K. R. Foster (2007). "Cooperation and conflict in microbial biofilms." Proc Natl Acad Sci U S A **104**(3): 876-881.
- Xavier, J. B., E. Martinez-Garcia, et al. (2009). "Social evolution of spatial patterns in bacterial biofilms: when conflict drives disorder." Am Nat **174**(1): 1-12.